TECHNOLOGIES TO ENHANCE THE OPERATION OF EXISTING NATURAL GAS COMPRESSION INFRASTRUCTURE

Quarterly Technical Progress Report

Reporting Period Start Date: 01/01/05
Reporting Period End Date: 03/31/05

Prepared by

Anthony J. Smalley
Ralph E. Harris
Gary D. Bourn
Danny M. Deffenbaugh

DOE Award No. DE-FC26-02NT41646
SwRI® Project No. 18.06223

Prepared for

U.S. Department of Energy
National Energy Technology Laboratory
3610 Collins Ferry Road
P.O. Box 880
Morgantown, WV 26507-0880

January 28, 2005

SOUTHWEST RESEARCH INSTITUTE®

SOUTHWEST RESEARCH INSTITUTE®
6220 Culebra Road
San Antonio, Texas 78238

TECHNOLOGIES TO ENHANCE THE OPERATION OF EXISTING NATURAL GAS COMPRESSION INFRASTRUCTURE

Quarterly Technical Progress Report

Reporting Period Start Date: 01/01/05
Reporting Period End Date: 03/31/05

Prepared by

Anthony J. Smalley
Ralph E. Harris
Gary D. Bourn
Danny M. Deffenbaugh

DOE Award No. DE-FC26-02NT41646
SwRI® Project No. 18.06223

Prepared for

U.S. Department of Energy
National Energy Technology Laboratory
3610 Collins Ferry Road
P.O. Box 880
Morgantown, WV 26507-0880

January 28, 2005

Approved:

Robert L. Bass, Vice President
Mechanical and Materials Engineering Division

SOUTHWEST RESEARCH INSTITUTE®

DISCLAIMER

This report was prepared as an account of work sponsored by an agency of the United States Government. Neither the United States nor any agency thereof, nor any of their employees, makes any warranty, express or implied, or assumes any legal liability or responsibility for the accuracy, completeness, or usefulness of any information, apparatus, product, or process disclosed, or represents that its use would not infringe privately owned rights. Reference herein to any specific commercial product, process, or service by trade name, trademark, manufacturer, or otherwise does not necessarily constitute or imply its endorsement, recommendation, or favoring by the United States Government or any agency thereof. The views and opinions of authors expressed herein do not necessarily state or reflect those of the United States Government or any agency thereof.

ABSTRACT

This quarterly report documents work performed under Tasks 15, 16, and 18 through 23 of the project entitled: *Technologies to Enhance the Operation of the Existing Natural Gas Compression Infrastructure*. The project objective is to develop and substantiate methods for operating integral engine/compressors in gas pipeline service, which reduce fuel consumption, increase capacity, and enhance mechanical integrity. The report first documents a survey test performed on an HBA-6 engine/compressor installed at Duke Energy's Bedford Compressor Station. This is one of several tests planned, which will emphasize identification and reduction of compressor losses. Additionally, this report presents a methodology for distinguishing losses in compressor attributable to valves, irreversibility in the compression process, and the attached piping (installation losses); it illustrates the methodology with data from the survey test. The report further presents the validation of the simulation model for the Air Balance tasks and outline of conceptual manifold designs.

TABLE OF CONTENTS

Section Page

LIST OF FIGURES

LIST OF FIGURES *(Cont'd)*

Figure Page

LIST OF FIGURES *(Cont'd)*

LIST OF TABLES

1. INTRODUCTION

This quarterly report presents results from a survey site test on an HBA-6 integral engine compressor, and methodology for distinguishing losses in the compressor cylinders, valves, and adjacent piping. The data from the site visit is used to illustrate and apply the methodology. As discussed, this is one of several tests to be directed at identifying and reducing losses in U.S. natural gas transmission compressor installations, thereby reducing fuel consumption and improving capacity of compressors operating at their power or torque limit.

1.1 THE U.S. GAS TRANSMISSION COMPRESSION INFRASTRUCTURE

The gas transmission industry operates over 4,000 integral engine compressors, which play a major role in pumping natural gas through the U.S. pipeline system. Although the use of centrifugal compressors in the U.S. pipeline industry has grown, these integral reciprocating units still represent over 70% of the fleet in numbers and over one-half of the installed power. These "slow-speed" integral engine compressors have been the workhorses of the industry for over 50 years, providing the reliable gas compression needed by the pipeline system. Figure 1-1 shows two such units: a 48-year old TLA6 and a 50-year old GMW10.

Figure 1-1. TLA6 (2,000 HP) and GMW10 (2,500 HP) in Pipeline Service

Figure 1-2 shows the age distribution of the current infrastructure. Over one-half of the fleet is well over 40 years old, but replacing all these units with currently available technology would incur a huge cost and disruption to service with insufficient improvement in overall performance of the pipeline system to justify this cost and disruption. For these reasons, wholesale replacement remains unlikely (although selective replacement driven by factors such as environmental regulations can be expected). Growth to a 30-TCF-plus gas market in the U.S., anticipated over the next 10 to 20 years, must come on the backs of the existing compression infrastructure; it will, therefore, depend on continued integrity, enhanced capacity, and efficiency of the existing integral engine/compressors under all loads. The industry needs demonstrated technology options and operating methods, which will cost-effectively maximize the capacity of these old units, and reduce their fuel consumption, while respecting or improving their integrity.

Figure 1-3, Figure 1-4, and Figure 1-5 exemplify these needs of the existing infrastructure.

Figure 1-3 shows how annual fuel consumption at individual compressor stations in the pipeline system varies with the number of horsepower hours delivered by the engine to the compressor cylinders at that station. Points on the high side of the mean slope represent stations, which are burning more than the industry average. In addition, with a regressed slope of 7.7 CF/BHP-Hr for Figure 1-3, the industry burns significantly more fuel than the most efficient current technology natural gas engines (as little as 6 CF/BHP-Hr). As a slightly different performance measure for the industry, Smalley, et al. [1], calculate an industry average (ratio of total fuel volume to total BHP-Hr) of 8.25 SCF/BHP-Hr.

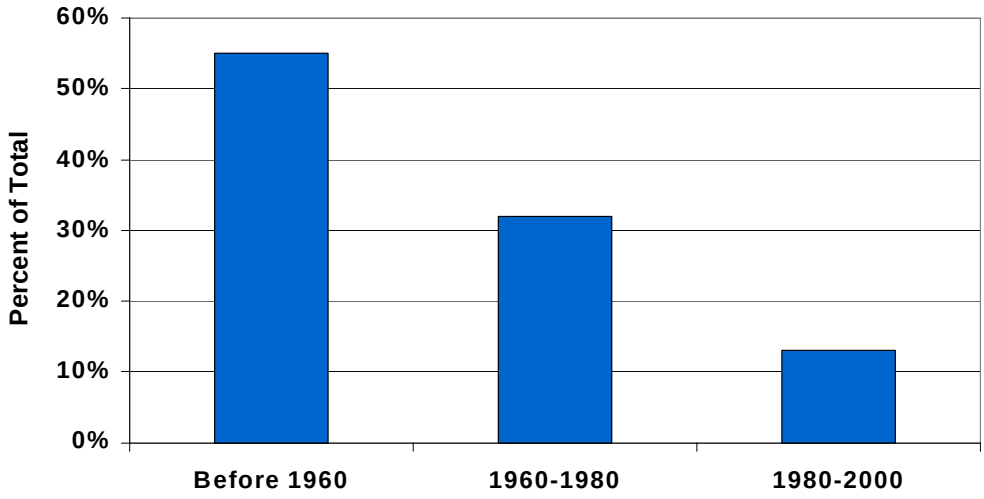

Figure 1-2. Install Dates: Over 50% of Pipeline Compressors Exceed 40 Years Old

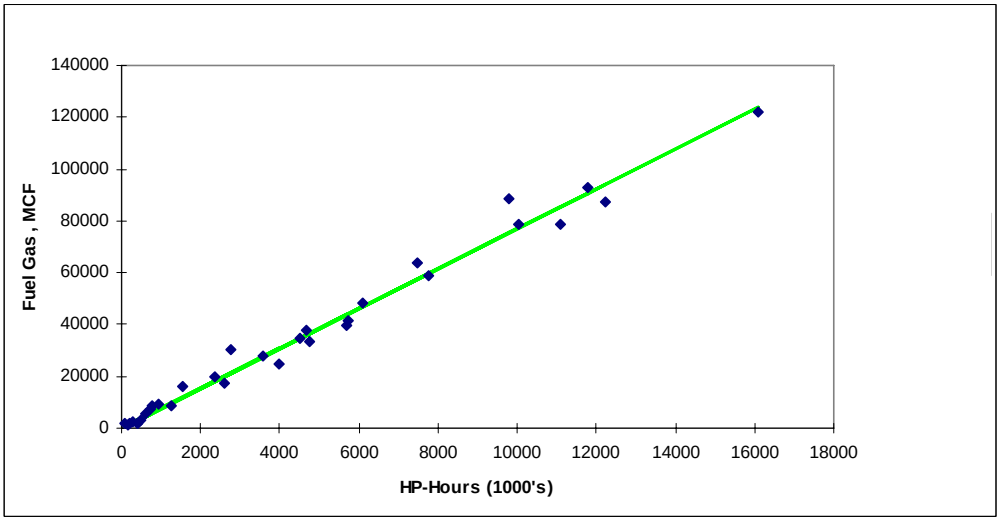

Figure 1-3. Industry Fuel Consumption
(~7.7 MCF/HP-Hr ±20% - Need to Lower the High Values)

Figure 1-4 presents a distribution of compressor thermal efficiency for the industry created by the Gas Machinery Research Council (GMRC) from a quantitative survey a number of years ago. This is the efficiency with which the compressors convert HP-Hr to useful compression. The width of the range and the 12 points by which the 79% median lies below the best achieved (91 to 92%) represents not only gas, which is burnt rather than delivered, but also engine capacity, which must overcome losses rather than deliver useful compression of the transported gas.

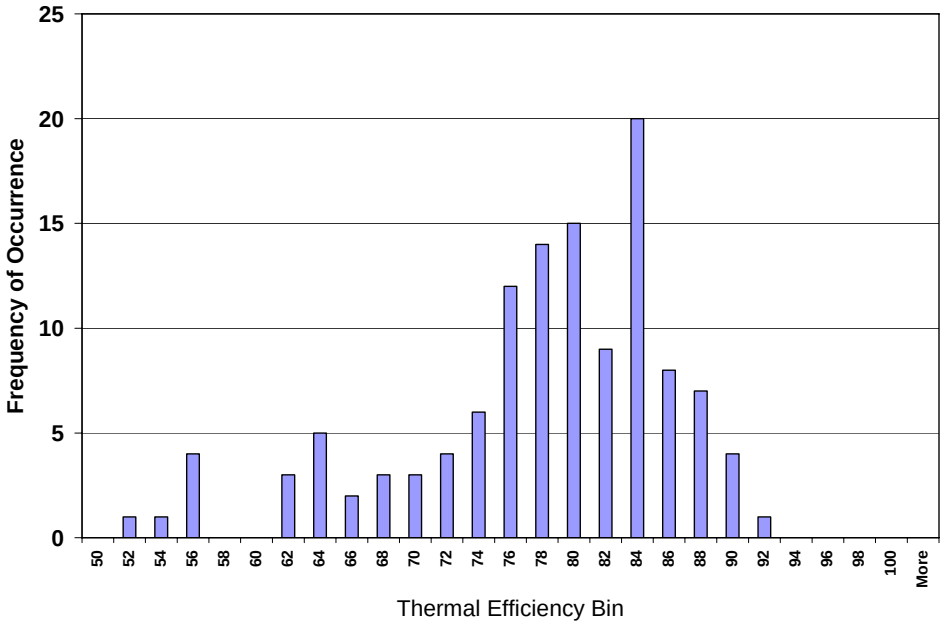

Figure 1-4. Compressor Thermal Efficiency Histogram Based on GMRC Survey

Figure 1-5 shows a number of failed crankshafts. This problem continues to occur at an undesirable rate for the pipeline industry as a whole (about one failure per thousand engines per year). This rate may not seem excessive, but for the compressor station and company, which incurs such a failure, the disruption, cost, and loss of capacity at the time is significant. The chance of this rate increasing as a penalty for improved performance and increased capacity must be avoided, as well as any increase in problems, such as bearing failure, or damage caused by detonation, or unintended overload.

Figure 1-5. Integrity: Crankshaft Failure Examples – Need Methods of Avoidance

1.2 THE COMPRESSION INFRASTRUCTURE PROJECT

Three years ago, the U.S. Department of Energy (DOE) initiated a Natural Gas Infrastructure (NGI) program whose goals included increasing capacity of the current pipeline infrastructure (10%) and reducing operational costs (50% by 2010). As part of this program, Southwest Research Institute® (SwRI®) is undertaking a project entitled, "Technologies to Enhance the Operation of Existing Natural Gas Compression Infrastructure." This project is managed for DOE by the National Energy Technology Laboratory (NETL). The project objective is:

> To develop and substantiate methods for operating integral engine/compressors in gas pipeline service that reduce *fuel consumption*, increase *capacity*, and enhance mechanical *integrity*.

1.3 PROJECT ACCOMPLISHMENT

This project continues to document and demonstrate feasibility of technologies and operational choices for companies who operate the large installed fleet of integral engine compressors in pipeline service. Applying project results will enhance integrity, extend life, improve efficiency, and increase capacity, while managing NO_x emissions. These benefits will translate into lower cost, more reliable gas transmission, and options for increasing deliverability from the existing infrastructure on high demand days. In the process, the project has assembled a powerful suite of instruments and a data system with which it has characterized behavior of the units tested under a wide range of conditions. This suite will remain available for characterization and optimization after completion of the project. The following documents its ongoing value and contribution to DOE goals.

1.3.1 Integrity

Increasing integrity and reducing statistical likelihood of component failure reduces transmission cost and enhances aggregate deliverability. Detonation represents a damaging threat to an engine. Applying the detonation detection technology tested under the project will mitigate this threat, which widely inhibits potentially beneficial operation with advanced timing. The newly defined CPR balancing method, which has proved quick and convenient to apply, will help equalize air/fuel ratio across cylinders and reduce the tendency to detonate. The low cost control method demonstrated for maintaining a global equivalence ratio set point provides another option for maximizing the margin between misfire and detonation limits and using commercially available controllers. The crank Strain Data Capture Module (SDCM) applied on all engines tested has shown its value for defining conditions when crank damage rate increases. Measuring crankshaft torsional velocity has complemented the SDCM, particularly in documenting the influence of speed changes, showing also that torsional velocity data respond detectably to loss of torque from a misfire. The Rod Load Monitor evaluated and enhanced on every major test so far promises to avoid overload of engines and resulting damage by improving consistency of load torque values used in load step control.

1.3.2 Efficiency

As much as three percent of the natural gas consumed goes toward fuel gas for engines and turbines to drive compressors. This fuel gas would cost $3 billion at current rates—the single most significant cost of gas transportation. Increasing the aggregate efficiency with which engine/compressors convert fuel energy into useful compression work will reduce this cost and leave more of the gas in the pipeline system available to the end user. The project has already documented how high-pressure fuel injection coupled with the addition of a turbocharger on old GMW engines reduces heat rate by about seven percent. The demonstrated air/fuel ratio control on a rich burn, carbureted, four-stroke engine can replace manual adjustment and use of indirect measurement, allowing optimization for minimum fuel, for minimum emissions without a three-way catalyst, or for optimum catalyst performance if one is installed. The Rod Load Monitor discussed previously will allow engine operation at the point of highest efficiency (100% torque), with greatly reduced risk of overload. The detonation detector will safely allow more efficient engine operation with timing advanced. Comparison of the heat rate *versus* load characteristic has revealed small potential benefits in brake thermal efficiency by applying CPR balancing. Project mapping of system efficiency has made clear the importance of considering both compressor and engine when evaluating how operational decisions will impact fuel conversion efficiency; speed/load combinations that favor heat rate may, at the same time, hurt compressor efficiency, so maximizing efficiency requires careful choices based on data. The project will continue to identify ways to enhance this efficiency, with emphasis on the compressor and pulsation control. The limitations in relying on differential indicated power for compressor efficiency calculations has emphasized the need for an effective method of measuring compressor flow and temperature rise. The project has also made clear the need for more information about mechanical losses and has added to this knowledge with a new interpretation of the rod load data. Valve leaks represent a significant loss of compressor efficiency system-wide. Engine/compressor operators know the sensitivity of temperature rise to valve leaks, but the project has re-emphasized this sensitivity; the data normalization and statistical process control techniques already promoted by McKee, et al. [2], would lend themselves very effectively to monitoring of cylinder temperature rise and associated decision making based on economic significance. The project has documented air imbalance between cylinders as a widespread condition that can limit combustion efficiency. New Tasks 15 and 16 are characterizing air imbalance in more detail and will seek cost-effective solutions.

1.3.3 Capacity

As discussed above, integrity enhancement and reduced component failure probability will enhance aggregate deliverability. In addition to improving the efficiency of fuel conversion, all increases in compressor efficiency will reduce the fraction of available engine power that must go to overcome losses and will, thereby, also add to deliverability. Tests so far have shown a compressor efficiency range from 84% to 91%, adding to an earlier GMRC survey with a range from 52% to 92%! The high compressor efficiency values found present a benchmark that will add greatly to system capacity if more widely achieved. The remainder of the project will seek to re-emphasize compressor efficiency by characterizing and reducing compressor losses, both mechanical and thermodynamic. Measurements of flow, temperature rise, and dynamic pressure in the cylinder nozzles (as well as in the cylinders themselves) will help quantify and characterize inherent thermodynamic losses—a first step in their reduction. Previous tests have

shown the likely contribution of pulsations to these losses, yet pulsation control methods, such as acoustic filters and orifices must also take account of associated resistive pressure losses.

1.4 FIELD TEST PROGRAM OVERVIEW

The tests and analyses have been performed so far on two different two-stroke engine models from two manufacturers and on one four-stroke engine model: a Cooper GMW10 with three compressor cylinders, a Dresser-Clark HBA-6T with four compressor cylinders, and an Ingersoll-Rand KVG103. The HBA is a straight six with a turbocharger. The GMW is a V-10 and has been tested both with and without the combination of a turbocharger and high-pressure fuel injection system. The KVG is a V-10 with three compressor cylinders. The engine selection was based on detailed quantitative analysis of the engine population using a database prepared for the pipeline industry, which shows all three of the tested models are in the top seven, measured by horsepower installed, and in the top six by number of units installed. Thus, marked diversity has been achieved in the process of testing three widely deployed engine models.

1.5 FUTURE PROJECT EMPHASIS

Observations from the project and from a 1990s GMRC survey (discussed previously) indicate that many low speed engine/compressor units have compressor efficiencies, which could be significantly increased. It is believed that the compressor manifold system and lateral piping between the unit and the headers contributes significantly to low compressor efficiency. On this basis, reducing installation losses (i.e., losses outside the compressor cylinder) represent an opportunity to improve compression efficiency in the U.S. pipeline system and, thereby, to increase system capacity (by reducing energy spent overcoming compressor and piping losses and making it available for useful compression work).

For the next project phase, SwRI seeks to locate a slow-peed integral engine compressor whose compressor thermal efficiency suggests significant room for improvement (mid-80's or below), and where it is reasonable to believe that a significant fraction of the losses occur in the installation piping, and could be eliminated by installation changes or changes in operational practice. The project will test the unit, with emphasis on characterizing compressor losses. After testing, SwRI plans to undertake a performance analysis as part of the project and identify installation and/or operational changes, which will improve compressor thermal efficiency. The host would be expected to make these changes. SwRI would then return to evaluate performance improvement.

With the help of the Industry Advisory Committee (IAC) for the project, SwRI has now identified a number of candidate low speed integral engine compressors. An initial screening process is being undertaken to select a single unit for intensive testing and analysis. This screening and selection process will include the following criteria:

- Some basis to expect improvements from installation changes or operational changes;
- Installed instrumentation to support initial further screening of thermal efficiency (e.g., suction pressure and temperature, discharge pressure, and temperature);

- Expressed willingness of host to undertake changes to compressor manifold system;
- No more than four and preferably three compressor cylinders;
- Relatively common engine model not previously tested under the project (e.g., TLA, TCV, GMV, GMVH, KVS).

It may not be possible to meet all of these criteria, but all are likely factors to be considered and evaluated. "Survey" screening site visits are planned, and the first of these has been completed at Duke Energy's Bedford Station. The results presented and discussed in this report include data from this first site visit, and the prototyping and illustration of a method for distinguishing the sources of losses in a compressor and its piping system. Once a site has been selected for more detailed test, redesign, and evaluation, the composition of the instrumentation suite will likely be changed to focus on compressor performance (with possible reduction in the number of instruments deployed on the engine).

2. EXPERIMENTAL

2.1 OVERVIEW

The majority of this section describes the suite of instruments, which have been used in tests so far for intensive testing of the power and compression sides of integral engine compressors. This description is included in this report for completeness and for reference. As discussed in the Introduction, a series of "survey" site visits are being undertaken with the purpose of providing information and test data which, when analyzed, will help guide selection of one site for further intensive testing with emphasis on efficiency and capacity of the compressor, its compressor manifold system, and its attached piping. The further intent of testing will be to guide changes to the installation and/or operation, which achieve observable improvements in compressor efficiency and capacity.

In the following list of sensors and data channels (Section 2.2), which comprises the full suite used in field tests so far, a pair of asterisks and specific discussion denote those from the full list which make up the much reduced set of sensors and data channels used for the "**survey site tests**."

An additional section (2.3) briefly summarizes changes in the instrumentation suite, which are under discussion for use in testing to emphasize compressor side performance.

2.2 SENSORS AND DATA CHANNELS FOR FIELD MEASUREMENT

Sensors and data acquisition capabilities have been assembled to record the following data on large integral engine compressors.

- ***Dynamic Pressure in the Compressor Cylinders* – These measurements are used for compressor horsepower and flow determination. Both ends of each compressor cylinder have been instrumented for dynamic pressure in each test series. The sensors are Sensotec piezo-restrictive transducers. They are calibrated prior to each test by deadweight loading to generate known force per unit area in the test fluid applied to the sensing element.

  For the **survey site tests** discussed in this report, "roving" pressure transducers are used. Rather than install, calibrate, checkout, and concurrently acquire data from a transducer on every end of every cylinder, data is acquired from one cylinder at a time, and then the set of transducers is removed from that cylinder and re-installed on the next cylinder to be tested. The benefit is a much faster set-up for a screening test; as a penalty for this benefit, data concurrency and longer term concurrent trending are lost.

- *Dynamic Pressure in the Engine Cylinders* – These measurements are used for engine horsepower determination, engine balancing, and to calculate engine statistics. All power cylinders have been instrumented for dynamic pressure in each test series. The sensors are Kistler quartz piezoelectric transducers. Because they are dynamic sensors, they are calibrated prior to each test by suddenly applied

deadweight loading to generate known force per unit area in the test fluid applied to the sensing element.

- *Dynamic Pressure in the Engine Air Intake Manifold* – These measurements are used to correlate dynamic effects in the inlet manifolds, which deliver air for each cylinder with the dynamic statistics within each cylinder. They also provide the time-averaged value for air manifold pressure whose influence on engine heat rate and emissions is assessed. Air manifolds have been instrumented in each test series. The sensors are Kistler piezo-resistive pressure transducers with factory provided calibration.

- *Dynamic Pressure in the Engine Exhaust Manifold* – These measurements are used to determine dynamic variation of pressure in the engine manifolds, which capture hot exhaust gas from each cylinder, and to correlate these dynamic pressure variations with the dynamics within each cylinder. The sensors are Kistler piezo-resistive transducers with factory provided calibration; they are water-cooled to reduce uncertainty resulting from temperature influence on the sensor readings. It has not been possible to install these transducers on exhaust manifolds with water jackets.

- *Torsional Vibrations (IRV)* – This measures the dynamic variation in speed of rotation of the flywheel. The sensor is a BEI 512 pulse encoder driven through a flexible coupling by a shaft connected by a friction drive to the flywheel. The frequency of its output pulse train directly reflects instantaneous flywheel angular velocity, which varies within each cycle of the engine because of dynamic load variation. Rather than digitally time the variation in the period between pulses (which imposes unrealistic period discrimination requirements), a frequency to voltage analog circuit is used to determine the continuous variation in flywheel speed. The frequency-to-voltage measurement is calibrated by supplying the analog circuitry with a pulse train of known frequency from a signal generator. The torsional vibration has been measured in this way on all tests. The torsional vibration data have been assessed as a potential indicator of engine dynamic loading severity.

- ***Data Acquisition Triggering* – The BEI encoder signal is also used to trigger acquisition of samples from all dynamic transducers. The phasing of the pulse train to top dead center is important. A pre-established top dead center mark for power Cylinder 1 is used as a reference, and the angular setting within the DAS corresponding to Cylinder 1 TDC is adjusted, as the engine runs, until a strobe light triggered by the DAS at this angle shows that the mark on the flywheel coincides with the stationary mark.

  The same encoder and triggering methodology are used for the **survey site tests** in conjunction with the transducer set installed on each cylinder in turn.

- *Bearing Centerline Vibration* – This measurement is assessed as an indicator of engine dynamic loading severity. The sensors are PCB velocimeters with factory provided calibration. The sensors have been located to measure lateral vibration at each end of the engine/compressor frame.

- *Crankshaft Dynamic Strain* – This measurement is used as a direct indicator of shaft loading, and to provide a link between engine statistical quantities and potential for crankshaft fatigue damage (Harris, et al. [3]). The strain gage is placed on the crankshaft web as close as possible to the crank pin—at the point most sensitive to opening and closing of the crank throw faces under load from engine and compressor rods. Data are acquired by the Strain Data Capture Module (SDCM), which rides on the shaft within the engine during each day of testing and from which data are downloaded at the end of each day. This is calibrated using a calibration resistance. The SDCM has worked with complete reliability for all tests so far. Its main drawback is the need for daily download, which can cut into test time; a refinement is under consideration that increases storage and energy capacity by a factor of ten or more.

- *Engine Fuel Flow* used to document overall engine efficiency – This sensor is an Emerson Flobas 103 transmitter that implements the AGA3 flow measurement based on a differential pressure measurement and is factory calibrated with a certificate. It is connected to taps on the already installed engine fuel flow orifice, which has been available on all engines tested so far. The fuel flow, coupled with a gas analysis, provides the basis for determining fuel energy consumed by the engine and for determining heat rate and overall system efficiency. At the first test, the flow measurement functioned, but the flow range was not properly matched to the engine, and satisfactory data was not obtained. At subsequent tests, the fuel flow has been successfully measured and used for the intended purposes.

- ***Pressures and Temperatures in Headers and Laterals (Suction, Discharge)* – These measurements are used for installation efficiency determination. Pressures are measured with Sensotec piezo-restrictive transducers. Permanently installed station sensors have been used to provide these data at some sites.

  For the **survey site tests** (and for several of the full scale tests undertaken), pressure and temperature data in the suction and discharge headers has been obtained from permanently installed station instruments. The standard station instruments are transmitters without dynamic pressure response capability, but when well calibrated, they provide accurate data on the operating conditions for the tested unit.

  To supplement cylinder pressure and station header pressure data, the **survey site test** reported herein has also used dynamic pressure measurement in the unit laterals and in the suction and discharge nozzles. This enables interaction of pressures at these locations and of cylinder power to be evaluated.

- *Engine Exhaust O_2 Level* – This measurement is used to determine global equivalence ratio, both as an independent variable influencing engine performance, and where the loop is closed to the turbocharger waste gate (two-stroke) or fuel rate valve (four-stroke) for active control. The sensor used is an NGK fast-response transducer, which provides a continuous variation of voltage with exhaust oxygen level. It is calibrated against a standard.

- *Engine Exhaust NO_x Level* – This measurement is used to provide comparative emissions data. The sensor used is an NGK fast-response transducer that provides a

continuous variation of voltage with exhaust NO_x level. It is calibrated against a standard.

- *Compressor Rod Load* – This measurement is used for both mechanical integrity and loading optimization. The sensor uses a pair of strain gages mounted on either side of the rod, which are bridged additively to cancel bending and to produce a signal proportional to axial load on the piston rod. The signal is transmitted using RF from a moving antenna to a stationary antenna. The strain gage and signal transmission can be powered by a battery or by a generator driven by rod motion. The battery power is adequate and simpler to set up for short-term tests, but for continuous monitoring and control, self-powering is needed. Calibration issues are not fully resolved yet for this device [termed the "Rod Load Monitor" (RLM)]. So far, the horsepower measurement from the compressor cylinder, based on cylinder pressure transducer, has been used for calibration.
- *Knock Detection* – This sensor, provided by Metrix, counts occurrences of dynamic acceleration levels above a threshold.

2.3 POTENTIAL INSTRUMENT CHANGES FOR COMPRESSOR SIDE TESTING

The following potential changes to the instrument suite make-up are under consideration for the remaining intensive testing in which it is planned to emphasize compressor side performance.

- *Nozzle Dynamic Pressure Measurement* – This has been discussed above in relation to the survey site tests. Knowledge of dynamic pressure variation in the nozzles acquired coherently with dynamic pressure variation in cylinder, laterals, and headers allows for more specific assessment of the time integrated pressure drop across the compressor valves between cylinder and nozzles, and also provides a reference for assessing pressure drop through compressor manifold and lateral piping between nozzles and headers. Effective interpretation of these pressures demands accurate and consistent calibration for all the pressure transducers involved.
- *Compressor Natural Gas Flow Measurement* – This is a very challenging measurement because of flow modulations and local noise, particularly if dynamic variation of flow over a compressor cycle is to be distinguished. If it can be accomplished, the knowledge will help define the influence of operational parameters on compressor capacity and will better define the power loss (flow weighted pressure drop) across sections of system piping.
- *Compressor Suction and Discharge Temperature Measurement* – This measurement is within the existing state of the art. A well-calibrated temperature measurement, coupled with reliable and co-located pressure measurement, with the knowledge of compressed gas composition and accurate thermophysical properties for the operating conditions, enables deviations from isentropic compression to be accurately assessed, and the influence of operational and configurational changes on these deviations to be evaluated.

- *Basis for Compressor Mechanical Loss Assessment* – The Rod Load Monitor evaluated at each detailed test undertaken so far has shown its potential for distinguishing the mechanical friction losses incurred by the compressor piston rings and rider bands. While piston friction is not readily amenable to design changes, the knowledge of how operation affects piston friction losses can become significant when operational changes are under consideration for other purposes.

2.4 LABORATORY GMVH MEASUREMENTS FOR AIR BALANCE TASKS

The GMVH engine was highly instrumented prior to utilization for the air balance investigation. However, additional dynamic pressure measurements were required for proper simulation with the computational model. The additional instrumentation is as follows:

- *Dynamic Pressure in Exhaust Manifold Runners* – Prior to the air balance investigation, only Cylinder 1L was instrumented for dynamic exhaust pressure. Additional dynamic pressure sensors were added to the remaining five cylinders to capture the dynamic pressure pulsations of the exhaust from each cylinder's ports. These sensors are of a thin-film strain gage type, typically used for absolute pressure measurement of manifold pressure in automotive electronic engine control systems. Each sensor was calibrated and a comparison test to a Kistler piezo-resistive sensor was performed on the running engine to validate transient response.
- *Dynamic Pressure in Exhaust Manifold Plenum* – A new sensor was installed in the exhaust manifold plenum near the turbocharger. This measurement is required to capture the dynamic pressure pulsations in the exhaust manifold plenum and provide data to characterize the dynamic flow through the exhaust manifold. A Kistler piezo-resistive absolute pressure transducer was utilized for this measurement. This sensor was calibrated via a deadweight tester. A photograph of the exhaust plenum sensor as installed for testing is provided in Figure 2-1.
- *Dynamic Pressure in Inlet Manifold Plenums* – Prior to the air balance investigation, only the left inlet manifold was instrumented for dynamic inlet plenum pressure. An additional dynamic pressure sensor was added to the right inlet manifold plenum to capture the dynamic pressure pulsations of the exhaust from each cylinder's ports. These sensors are of a thin-film strain gage type, like those utilized in the exhaust manifold runners.

The complete instrumentation package on the laboratory GMVH engine is listed in Table 2-1.

In addition to the many measurements for engine performance and emissions, several static measurements were made of the engine geometry. These geometric measurements have been determined to be of critical importance for proper simulation of the engine. The key geometric parameters to be determined are compression ratio, port timing, and port area in each cylinder of the test engine. In order to conduct the many detailed measurements, the engine was disassembled. A list of the many static measurements taken on each cylinder is provided in Table 2-2. From these measurements, several calculated parameters were derived and discussed in the next section.

Table 2-1. Time-Averaged and Crank-Angle Resolved Measurements on GMVH

Time-Averaged Measurements	
Engine Speed	Oil Pressure
Turbocharger Shaft Speed	Turbocharger Oil Pressure
Turbocharger Wastegate Position	Coolant Inlet & Outlet Pressure
Engine Torque	Pre-Turbine Pressure
Total Fuel Flow	Stack Pressure
Pre-Chamber Fuel Flow	Compressor Inlet Temperature
Fuel Gas Composition	Compressor Left & Right Outlet Temperatures
Fuel Gas Heating Value	Inlet Manifold Left & Right Temperatures
Total Air Flow	Fuel Header Temperature
Barometric Pressure	Pre-Chamber Header Temperature
Ambient Temperature	Individual Cyl. Exhaust Runner Temperatures
Ambient Humidity	Pre-Turbine Temperature
Exhaust NOx Concentration	Post-Turbine Temperature
Exhaust CO Concentration	I/C Inlet Left & Right Water Temperatures
Exhaust HC Concentration	I/C Outlet Left & Right Water Temperatures
Exhaust CO2 Concentration	Oil Sump Temperature
Exhaust O2 Concentration	Oil Inlet Temperature
Exhaust Equivalence Ratio	Turbocharger Oil Inlet Temperature
Inlet Manifold Left & Right Pressures	Coolant Inlet & Outlet Temperatures
Fuel Header Pressure	Individual Cyl. Head Temperatures
Pre-Chamber Header Pressure	Dynomometer Inlet & Outlet Temperatures
Crank-Angle Resolved (Dynamic) Measurements	
Cylinder 1L Firing Pressure	Cylinder 1L Exhaust Runner Pressure
Cylinder 2L Firing Pressure	Cylinder 2L Exhaust Runner Pressure
Cylinder 3L Firing Pressure	Cylinder 3L Exhaust Runner Pressure
Cylinder 1R Firing Pressure	Cylinder 1R Exhaust Runner Pressure
Cylinder 2R Firing Pressure	Cylinder 2R Exhaust Runner Pressure
Cylinder 3R Firing Pressure	Cylinder 3R Exhaust Runner Pressure
Left Inlet Manifold Plenum Pressure	Right Inlet Manifold Plenum Pressure
Cylinder 1L Pre-Chamber Firing Pressure	Exhaust Manifold Plenum Pressure

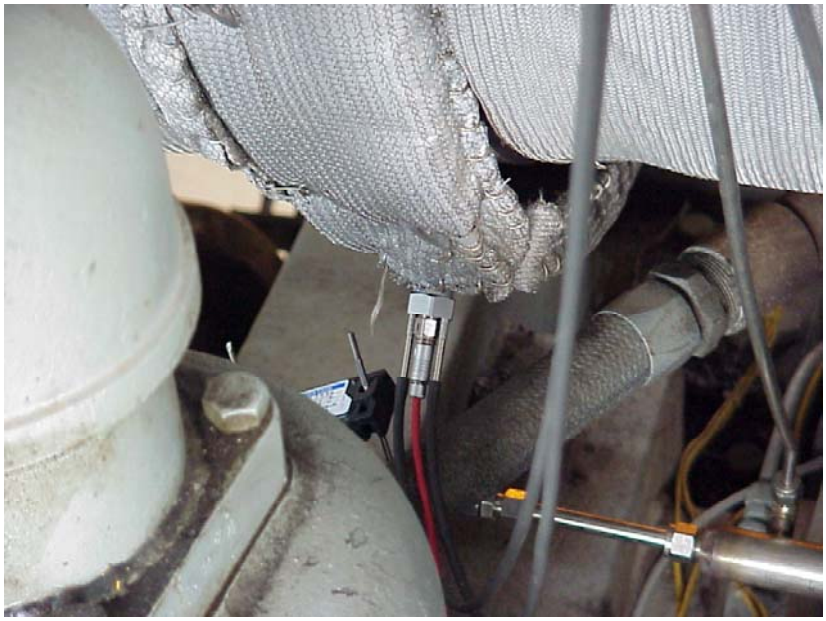

Figure 2-1. Photograph of Dynamic Exhaust Pressure Sensor in Exhaust Plenum

Table 2-2. Static Measurements on Each Cylinder of GMVH

Piston Stroke (BDC to TDC)	Cylinder Bore (~1" from top)
Connecting Rod C-C (cyl 1L only)	Piston TDC Height (from cylinder top)
Pre-Chamber Volume	Piston Top Ring Land Diameter
Cylinder Inlet Volume (inc.ports)	Piston Top Ring Land Height
Cylinder Intake Flange Width	Piston Dome Angle
Cylinder Intake Flange Height	Piston Dome Height from edge
Cylinder Exhaust Flange Width	Piston Bowl Depth
Cylinder Exhaust Flange Height	Piston Bowl Volume (inc puller-hole)
Cylinder Head Volume	Piston Pin Center to Crown Height
Cylinder Head Gasket Step	Top Int Port to Gasket Step - A
Cylinder Head Gasket Thickness	Top Int Port to Gasket Step - B
Exhaust Port "Shape" - A	Top Int Port to Gasket Step - C
Exhaust Port "Shape" - B	Top Int Port to Gasket Step - D
Exhaust Port "Shape" - C	Top Int Port to Gasket Step - E
Exhaust Port "Shape" - D	Top Int Port to Gasket Step - F
Exhaust Port "Shape" - E	Top Int Port to Gasket Step - G
Top Exh Port to Gasket Step - A	Top Int Port to Gasket Step - H
Top Exh Port to Gasket Step - B	Intake Port to Edge Width - A
Top Exh Port to Gasket Step - C	Intake Port to Edge Width - B
Top Exh Port to Gasket Step - D	Intake Port to Edge Width - C
Top Exh Port to Gasket Step - E	Intake Port to Edge Width - D
Exhaust Port Edge Width - A	Intake Port to Edge Width - E
Exhaust Port Edge Width - B	Intake Port to Edge Width - F
Exhaust Port Edge Width - C	Intake Port to Edge Width - G
Exhaust Port Edge Width - D	Intake Port to Edge Width - H
Exhaust Port Edge Width - E	Intake Port Edge Height - A
Exhaust Port Min Width - A	Intake Port Edge Height - B
Exhaust Port Min Width - B	Intake Port Edge Height - C
Exhaust Port Min Width - C	Intake Port Edge Height - D
Exhaust Port Min Width - D	Intake Port Edge Height - E
Exhaust Port Min Width - E	Intake Port Edge Height - F
Exhaust Port Edge Height - A	Intake Port Edge Height - G
Exhaust Port Edge Height - B	Intake Port Edge Height - H
Exhaust Port Edge Height - C	Intake Port Angle - A
Exhaust Port Edge Height - D	Intake Port Angle - B
Exhaust Port Edge Height - E	Intake Port Angle - C
Exhaust Port Min Height - A	Intake Port Angle - D
Exhaust Port Min Height - B	Intake Port Angle - E
Exhaust Port Min Height - C	Intake Port Angle - F
Exhaust Port Min Height - D	Intake Port Angle - G
Exhaust Port Min Height - E	Intake Port Angle - H

Two of the six cylinders, representing a high and low compression pressure on a given bank, were to be flow tested. During disassembly, it was found that Cylinder 1R had a different exhaust port shape from the other cylinders and was removed to be flow tested. Therefore, Cylinders 1L, 3L, and 1R were removed from the engine. The flow testing was conducted to measure the discharge coefficient of both intake and exhaust ports versus open area. Accurate discharge coefficients are required for accurate simulation. In addition, a review of allowable port shape on the manufacturing drawings gave concern that variance in port shape from cylinder-to-cylinder could be a large contributor to flow imbalance. The effects of port shape also needed to be characterized and accounted for in the simulations.

A flow test rig was assembled specifically for this effort. This test rig featured a compressed air storage and regulation system, meter run, data acquisition, and cylinder stand. Photographs of the flow bench rig are shown together in Figure 2-2. The compressed air system featured three 1,050-gallon cylinders charged to 250 PSIG. The outlet of the compressed air cylinders was connected to a regulator and control valve for setting the desired pressure versus mass flow of air into the flow bench. The meter run was fabricated from Schedule 40 PVC pipe and featured an ASME nozzle for flow measurement. Two sizes of flow nozzles, 2- and 4-inch, were interchangeably used for low and high flows. Mass flow was calculated from the volumetric flow measurements using standard equations given in ASME codes. The cylinder stand was fabricated to hold and seal the cylinder during testing. An adjusting screw protruded from the bottom of the stand to allow for adjustment of piston height to achieve the desired port open fraction. A Vernier scale mounted on the bottom of the stand was used for measuring piston travel. A fixture was later fabricated to mount on the cylinder studs to lock the piston and prevent lifting due to air pressure leaking past the rings and under the piston. The data acquisition system acquired data at a rate of 6 Hz and included the measurements given in Table 2-3.

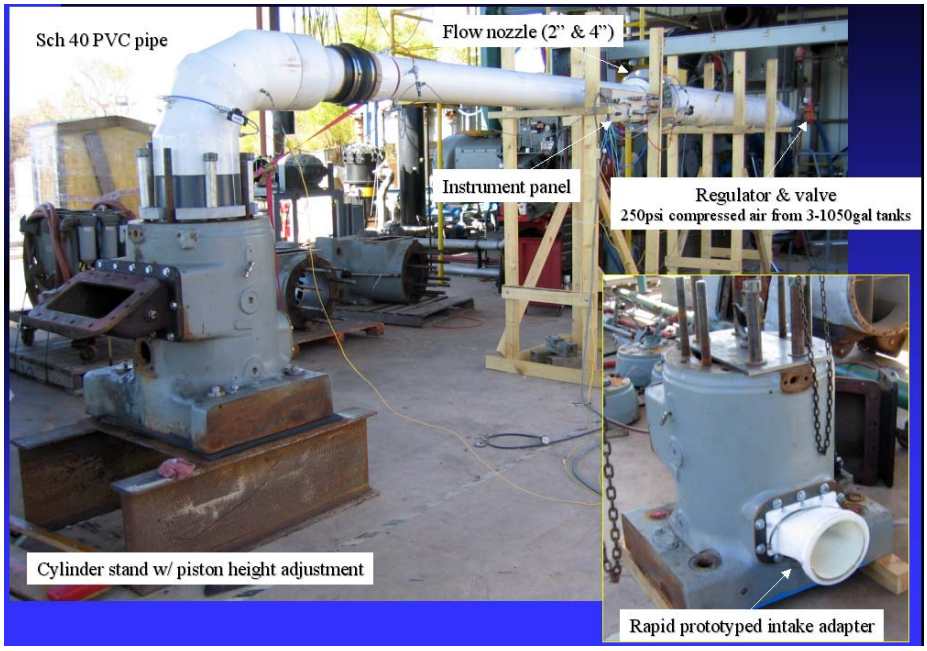

Figure 2-2. Photographs of GMVH Cylinder Flow Bench

Table 2-3. GMVH Cylinder Flow Bench Measurements

Supply Static Pressure (upstream)	Ambient Pressure
Supply Temperature (upstream)	Ambient Temperature
4" Nozzle delta-Pressure	Ambient Dewpoint Temperature
2" Nozzle delta-Pressure	Air Tank Pressure
Plenum Static Pressure (downstream)	Piston Travel from BDC
Plenum Temperature (downstream)	

Results from recent simulations with the additional measurements incorporated have shown that the actual inlet air temperature, passing through the ports, is significantly hotter than that measured in the inlet manifold. This increased inlet air temperature is due to a portion of the air mass coming from the large plenum in the base, where the air is heated closer to oil temperature. Additional temperature sensors have been installed directly into the air box of two cylinders to validate the model predictions of elevated inlet air temperature.

2.5 COMPUTATIONAL MODELING FOR AIR BALANCE INVESTIGATION

The computational modeling for the air balance investigation is being performed with software purchased from Optimum Power Technology. The particular software package is titled *Automated Design with Virtual 2-Stroke*. This software is a one-dimensional cycle-simulation model that focuses on the fluid dynamics in an internal combustion engine.

A model of the GMVH engine was configured using the dimensions provided by Cooper Compression and obtained through direct measurement. Being a one-dimensional computational model, many of the complex three-dimensional geometries were simplified to representative pipes, plenums, junctions, and orifices. A schematic of the current computational model of the GMVH-6 engine is provided in Figure 2-3. This model now incorporates the base plenum and more precise geometric dimensions derived during engine teardown.

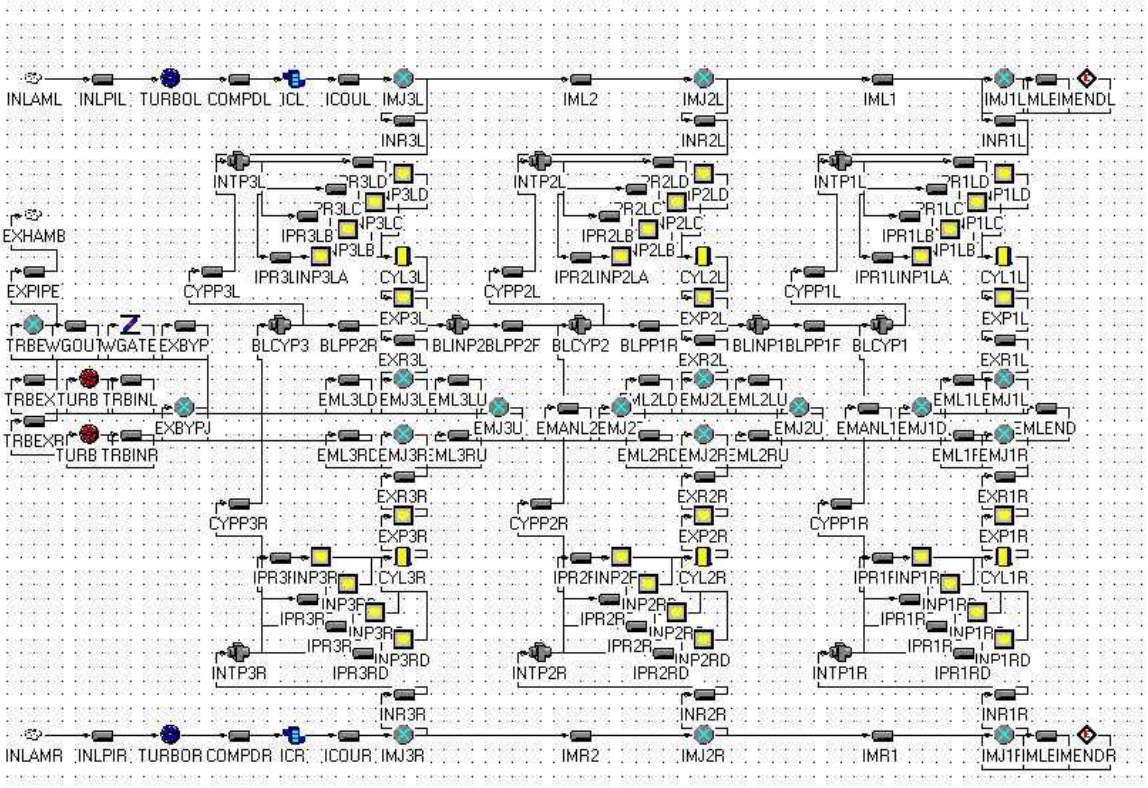

Figure 2-3. Current GMVH Computational Model Schematic

3. DATA ACQUISITION

3.1 FIELD DATA SYSTEM

Figure 3-1 and Figure 3-2 show photographs of the Field Data Acquisition System (DAS). The system comprises an industrially hardened computer, a flat screen for display, and a separate box with connectors to which cables from individual sensors are connected. The DAS box has analog-to-digital converters of appropriate speed for over 50 different channels.

Figure 3-1. Front View of Field Data Acquisition System (DAS)

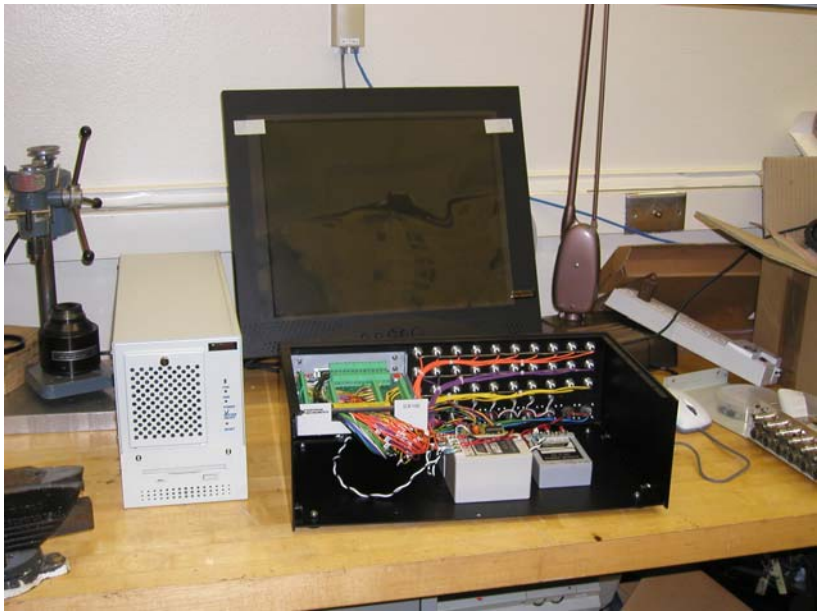

Figure 3-2. Rear View of Field Data Acquisition System (DAS)

The individual power cylinder transducers (up to 10) are connected to a box with connectors on the deck near the cylinders. A single cable from this box carries the signals from all the power cylinder transducers to the main data acquisition box. A similar approach is used for the compressor cylinders. In this way, the complexity of the cabling and system checkout is minimized. Signals from rod load monitors from other system pressures and from temperature sensors are acquired by the DAS, concurrently, and a database of the sensor values throughout each test is created by the DAS.

3.2 DATA ACQUISITION FOR SURVEY SITE TESTS

A PC-based data acquisition system is being used for the survey site tests. This system does not have the extensive channel capacity of the data acquisition system used in detailed testing at sites documented in previous reports. However, it is adequate for the reduced number of channels required for concurrent data acquisition on cylinder head- and crank-end, suction nozzle, discharge nozzle, and suction and discharge laterals (i.e., 6 channels). A transducer "break-out" box is used, which conditions the signal from the pressure transducers, together with an analog to digital (A to D) converter between the break-out box and the computer. Sampling by the A to D card is triggered by pulses from the encoder, which is driven by a quill shaft connected to the crankshaft at the flywheel.

The processing software is identical to that used by the higher capacity system in previous tests. Normally, this software is designed to acquire data at 512 angular subdivisions of 360 degrees of rotation, over 32 successive revolutions of the crankshaft, and to average the 32 values obtained at each of the 512 rotation angles. This averaging or "comb-filtering" process tends to minimize or eliminate random cycle-to-cycle variations and to reinforce persistent characteristics of the pressure variations.

During the first survey site test, the need was identified to characterize systematic variation in the pressure data, which was occurring at a slow frequency (fractions of a Hz). The averaging process, which normally aids the data acquisition process, was found to work against the need for this characterization, and a field modification was made to allow the capture and storage and analysis of individual pressure records, yielding information on how instantaneous power and pulsations were varying.

3.3 LABORATORY GMVH ENGINE

A photograph of the laboratory GMVH instrumentation and control panel is depicted in Figure 3-3. The data acquisition system is PC-based, and features custom software written by SwRI. In addition to recording and displaying the measurements listed in Section 2.4, the data acquisition software is programmed with many calculated parameters that are displayed in real-time for monitoring performance and setting specific operating conditions.

Figure 3-3. Laboratory GMVH Instrumentation and Control Panel

4. RESULTS AND DISCUSSION: SURVEY TEST ON AN HBA-6

4.1 OVERVIEW AND BACKGROUND TO TEST

Under the next phase of the compression infrastructure project, SwRI seeks to locate a slow-speed integral engine compressor whose compressor thermal efficiency suggests significant room for improvement (mid-80's or below), and where it is reasonable to believe that a significant fraction of the compressor losses occur in the installation piping, and could be eliminated by installation changes or changes in operational practice. The project will test the unit, with emphasis on characterizing compressor losses. After testing, SwRI plans to undertake a performance analysis as part of the project and identify installation and/or operational changes, which will improve compressor thermal efficiency. The host would be expected to make these changes. SwRI would then return to evaluate performance improvement.

With the help of the Industry Advisory Committee (IAC), SwRI has now identified a number of candidate low speed integral engine compressors. An initial screening process is being undertaken to select a single unit for intensive testing and analysis. This screening and selection process will include the following criteria:

- Some basis to expect improvements from installation changes or operational changes;
- Installed instrumentation to support initial further screening of thermal efficiency (e.g., suction pressure and temperature, discharge pressure, and temperature);
- Expressed willingness of host to undertake changes to compressor manifold system;
- No more than four and preferably three compressor cylinders;
- Relatively common engine model not previously tested under the project (e.g., TLA, TCV, GMV, GMVH, KVS).

With reference to the first two of these criteria, survey site visits and tests are being undertaken, and data from the first of these survey site visits and tests is presented and discussed here.

The site for the first survey test was Duke Energy's Bedford Station, with nine HBA-6 units. Since the original installation of these integral reciprocating engine compressors, two centrifugal compressors have been added at the station with electric motor drives. Operating conditions at the station have changed, with an increase in nominal discharge pressure from 800 PSIG to 1,000 PSIG. To accommodate this change without overloading the individual reciprocating compressor units, the capability to deactivate one end on one or more compressor cylinders has been added.

Double-acting compressor cylinders compress gas on both the outwards stroke when the piston moves away from the crankshaft and on the inwards stroke when the piston moves towards the crankshaft. Both ends (head-end and crank-end) are nominally similar (differing in swept area only by the area of the piston rod). Under double-acting operation, the inwards and outwards compression strokes tend to self-balance each other, thereby minimizing the magnitude

of flow pulses into the piping system at rotational frequency and leaving the lowest significant pulsation excitation frequency at twice rotational speed. Deactivating one end of a cylinder (single-acting operation) eliminates this balance and causes a much higher excitation at one times the rotational speed.

The pulsation filter bottles installed on these units were designed for only double-acting operation (this reduces filter size requirements). Since the configurational and operational changes, and the much more frequent occurrence of single-acting operation on these units, pulsations have been of concern, and performance has been observed to deteriorate.

4.2 SURVEY SITE TEST OVERVIEW

On March 1, 2005, a survey site test was performed on Unit 4 at Duke Energy's Bedford Station. The other units were running while the tests were conducted. Figure 4-1 shows the outside of the compressor building on the day of testing, with the stacks from four of the engines visible. The snow on the ground is apparent in Figure 4-1 where temperatures were in the 20's. The unit has four compressor cylinders as shown in Figure 4-2 and Figure 4-3. Testing was planned and implemented to acquire dynamic pressure data from head-end, crank-end, suction nozzle, and discharge nozzle on each of the four cylinders in turn, with data acquisition triggered by a 512-pulse encoder rotating with the crankshaft. In addition to these four transducers, which were moved from cylinder-to-cylinder, data was acquired during each cylinder test from pressure transducers installed on the suction and discharge lateral piping between the unit and the station headers for the nine units. Figure 4-4 shows the two pressure transducers installed on the lateral piping.

Figure 4-1. Photograph of Compressor Building Showing Unit Stacks (Duke Energy's Bedford Station; March 1, 2005)

Figure 4-2. Overview Photograph of Clark HBA-6 Compressor Cylinders (Duke Energy's Bedford Station; March 1, 2005)

Figure 4-3. Close-up of Compressor Cylinder; Clark HBA-6 Unit (Duke Energy's Bedford Station; March 1, 2005)

Figure 4-4. Installation of Header Pressure Transducers; Clark HBA-6 Unit 4 (Duke Energy's Bedford Station; March 1, 2005)

Testing started with Cylinders 1 and 4 in single-acting mode (head-ends deactivated on both these two cylinders). Pipeline conditions dictated single-acting operation to avoid overload. All the other units were running in the same configuration (according to standard procedure at the station). Initial observations indicated a systematic lack of repeatability in the data. Based on the nature of the observed variation, it was suspected that significant flow modulations at one times the rotational speed, coupled with small speed differences between units, were leading to a beating phenomenon (in which small differences in pulsation excitation frequencies from individual units give rise to a low frequency, repeated, growth and decay of pulsations at a frequency equal to the difference in excitation frequencies). A field change in the data acquisition software (discussed in Section 3 of the report) enabled the acquisition of pressure records at a rate of about one every two seconds, followed by individual analysis of each record for power, speed, and pulsation characteristics, so that the time variation of these characteristics could be observed.

After two to three hours of testing under single-acting conditions, changes were implemented to allow double-acting on all cylinders. At the prevailing pipeline conditions, double-acting operation would have overloaded the units, so in cooperation with neighboring stations, two units were taken off-line at Bedford. This steadily increased line pack upstream and decreased it downstream, so reducing the pressure ratio across the station, until after about 40 minutes the ratio stabilized at about 1.2 and all ends could be activated, avoiding the single-acting condition. The data under double-acting operation was much more stable as results will show. Isentropic efficiency data and horsepower per unit flow data also indicate that double-acting operation reduces compressor system losses.

The following sections present the data and exemplify the characteristics discussed above.

4.3 OPERATING CONDITION DATA

Figure 4-5 presents pressure data acquired from the permanently installed station instruments in discharge and suction headers. The suction pressure is in the range from 770 to 780 PSIG during most of the morning's testing. The discharge pressure is in the range of 980 to 990 PSIG. Shortly before 12:00 noon, two units out of nine were taken off-line; both suction and discharge pressures can be seen to start changing immediately, and they reach a near stable condition at about 800 and 960 PSIG, respectively. Figure 4-6 shows the corresponding compression ratio (ratio of discharge to suction absolute pressure) variation during the tests. The test data to be presented subsequently was obtained during the condition of stable values for ratio (1.28 during single-acting tests and 1.2 during double-acting tests) seen in Figure 4-6.

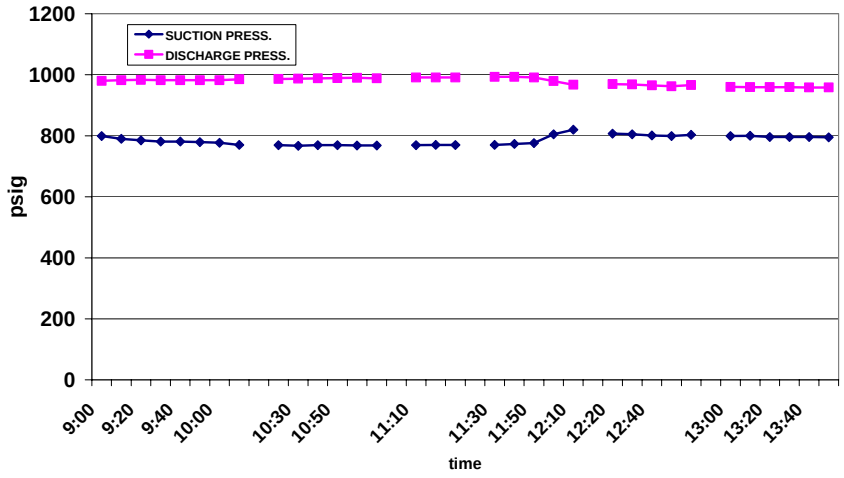

Figure 4-5. Variation of Suction and Discharge Pressure During Survey Site Test; Clark HBA-6 Unit (Duke Energy's Bedford Station; March 1, 2005)

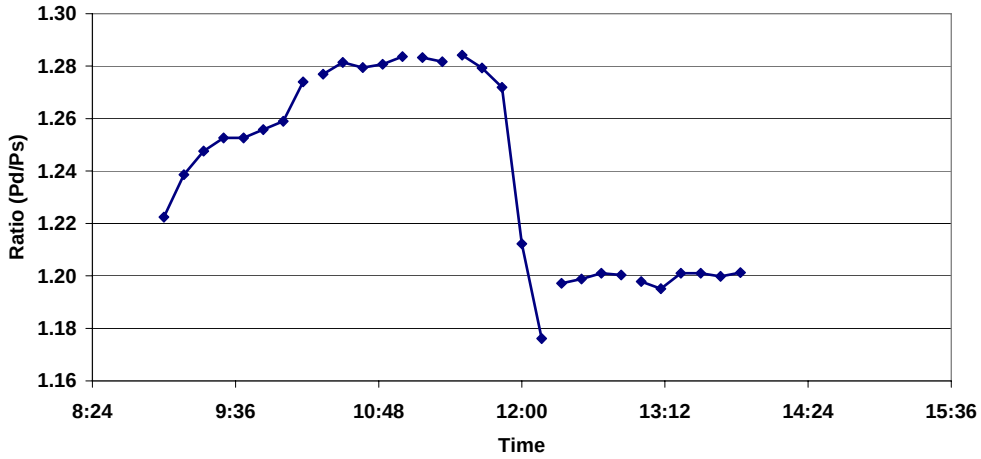

Figure 4-6. Variation of Pressure Ratio During Survey Site Test; Clark HBA-6 Unit (Duke Energy's Bedford Station; March 1, 2005)

Figure 4-7 shows the variation of temperatures during the day. Suction temperature remained relatively constant in the range of 49°F to 51°F, while discharge temperature reflects the changes in ratio, rising during the early part of the day, holding constant around 86°F during the single-acting tests, then dropping and holding around 77°F during the double-acting tests.

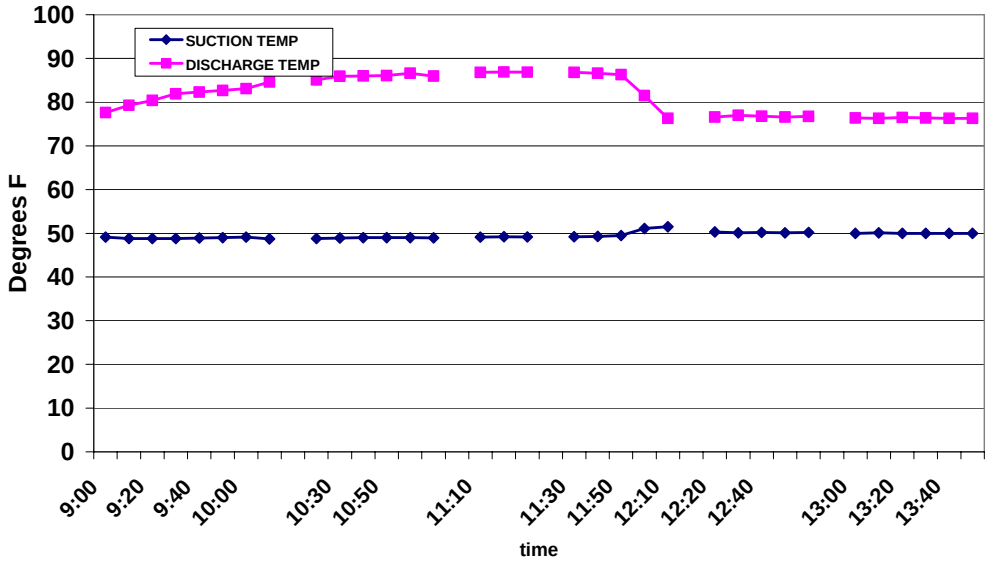

Figure 4-7. Variation of Suction and Discharge Temperature During Survey Site Test; Clark HBA-6 Unit (Duke Energy's Bedford Station; March 1, 2005)

4.4 CYLINDER PRESSURE DATA

As discussed above, the pressure and compressor performance characteristics were observed to vary with time under single-acting conditions (with Cylinders 1 and 4 head-ends deactivated). The first five frames of Figure 4-8 show Cylinder 1 pressure versus crank angle data at five successive points in time over a 75-second period (T = 0, 23, 42, 57, and 75 seconds). The sixth frame presents a 32-cycle average. Close inspection of the first five individual frames shows distinct variation over the test period—for example, in the relative height of the three peak pressure values during the discharge event of the crank-end (red) cylinder data and in the peak-to-peak range of the black line (head-end cylinder data). Since only Cylinders 1 and 4 are deactivated, it might be expected that the cycle-to-cycle variation would be limited to Cylinders 1 and 4. However, Figure 4-9 shows that Cylinder 2 (itself double-acting throughout these tests) also exhibits pronounced variation in both head-end (black) and crank-end (red) data over the five frames (T = 0, 1, 5, 40, and 57 seconds).

4.5 VARIATION OF CALCULATED POWER WITH TIME

Figure 4-10 shows how the calculated horsepower and speed for Cylinder 1 varies with time over a 51-second testing period from 10:57:31 to 10:58:22. The horsepower in particular shows a distinctly periodic variation, completing about eight cycles in 42 seconds, for an average period of about five seconds. The amplitude of power variation is about 20 HP peak-to-peak, which is well over 10% of the 180 HP mean power for this single-acting cylinder.

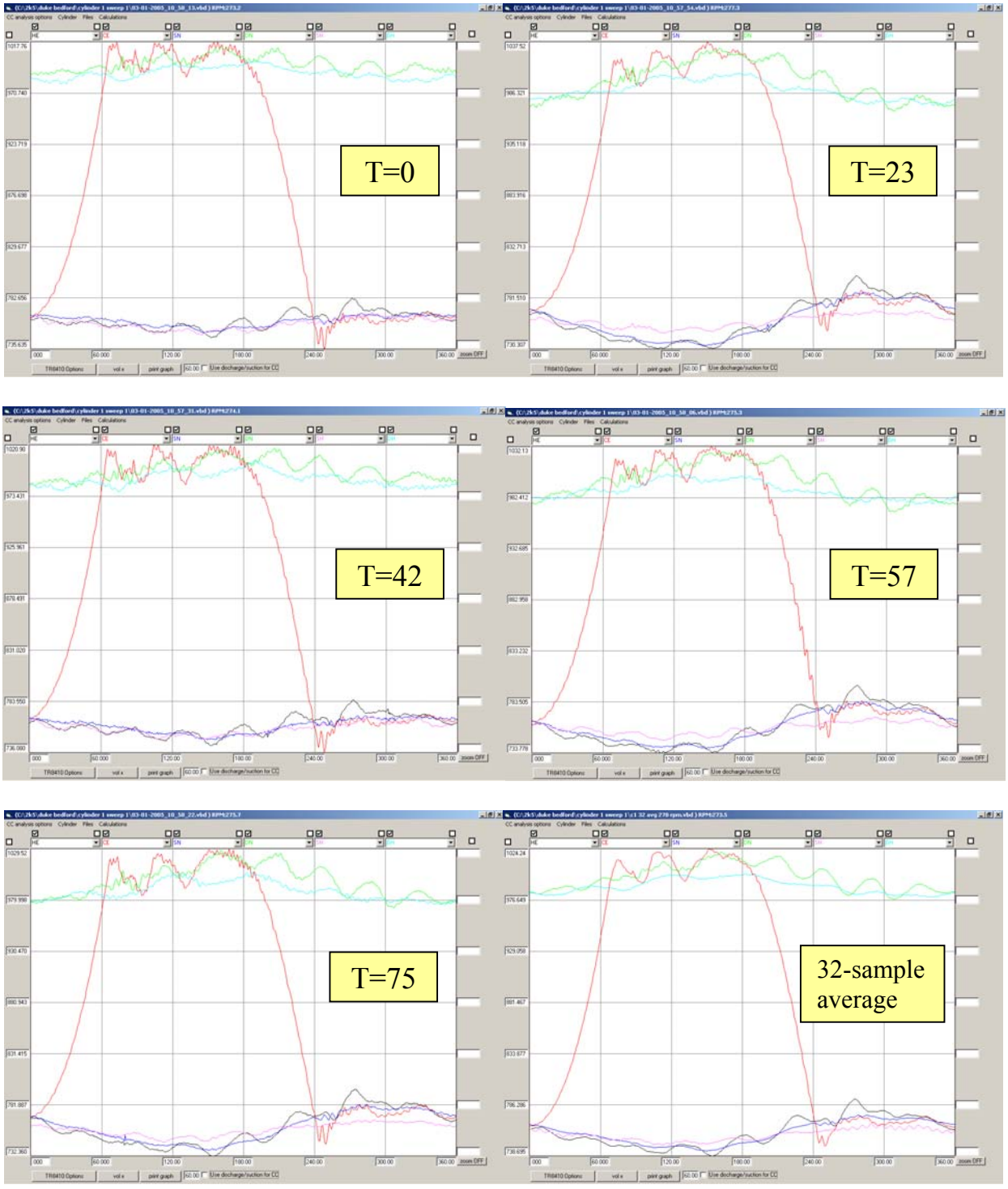

Figure 4-8. Successive Pressure-Crank Angle Data for Cylinder 1 Under Single-Acting Conditions for Cylinders 1 and 4; Head- and Crank-End Pressures; Nozzle Pressures and Unit Lateral Pressures at 0, 23, 42, 57, and 75 Seconds, Together with 32-Sample Average; Clark HBA-6 Unit 4 (Duke Energy's Bedford Station; March 1, 2005)

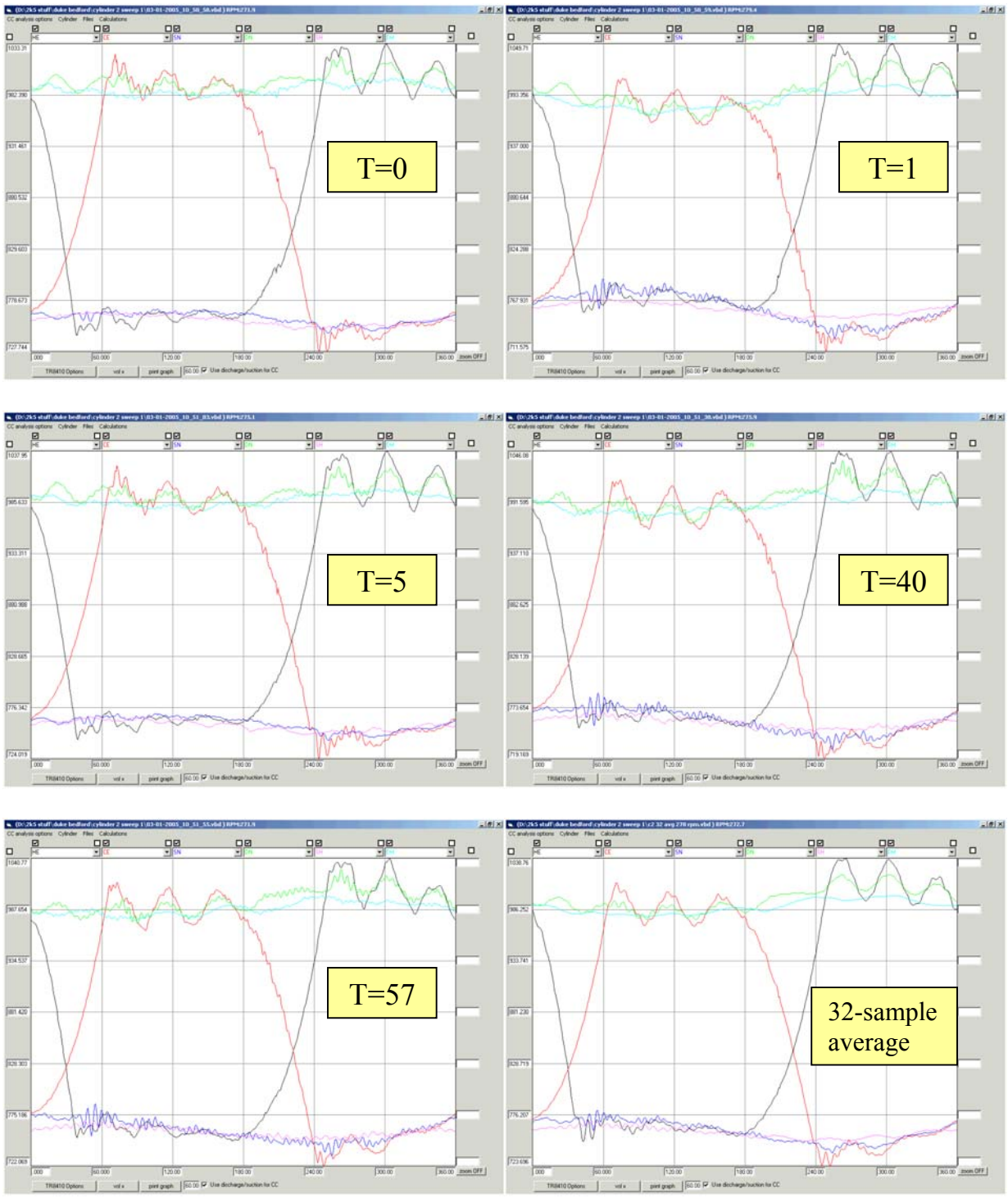

Figure 4-9. Successive Pressure-Crank Angle Data for Cylinder 2 Under Single-Acting Conditions for Cylinders 1 and 4; Head- and Crank-End Pressures; Nozzle Pressures and Unit Lateral Pressures at 0, 1, 5, 40, and 57 Seconds, Together with 32-Sample Average; Clark HBA-6 Unit 4 (Duke Energy's Bedford Station; March 1, 2005)

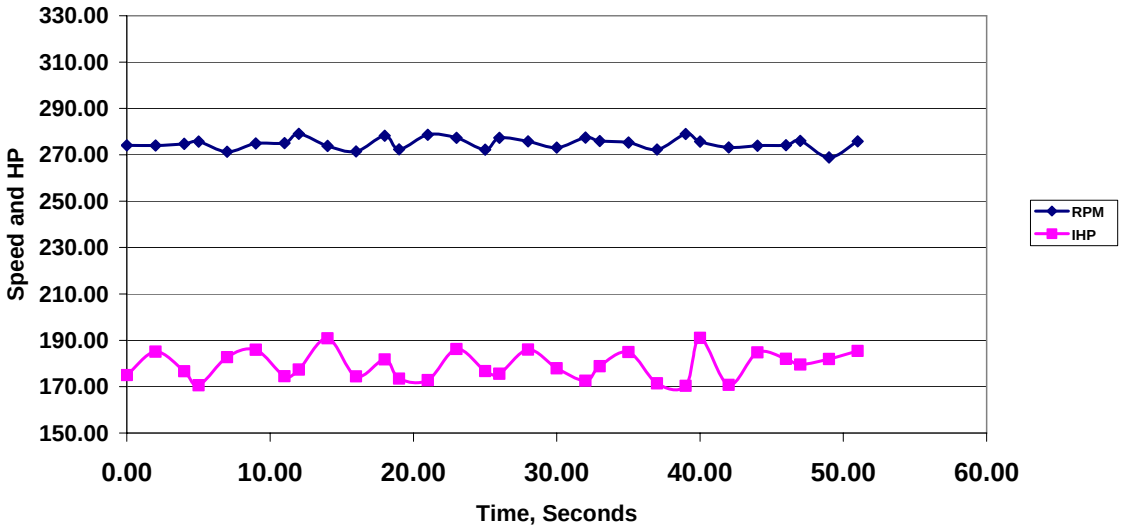

Figure 4-10. Cylinder 1 Speed and HP vs. Time, with Cylinders 1 and 4 Single-Acting; Clark HBA-6 Unit 4 Compressor Cylinders (Duke Energy's Bedford Station; March 1, 2005)

The speed displays a variation with a somewhat periodic nature and effective period similar to the power variation. The range of variation is about 8 RPM or 3% of the 275-RPM average speed.

Cylinder 3—itself double-acting, while Cylinders 1 and 4 are single-acting, exhibits pronounced variation of power with time and a similar periodicity to this variation as Cylinder 1 (Figure 4-11). The HP range is about 28—that is over 7.5% of the 365 HP average for this cylinder. As in Figure 4-10 for Cylinder 1, the speed shows about 8 RPM variation. Speed is a system characteristic, so this is to be expected.

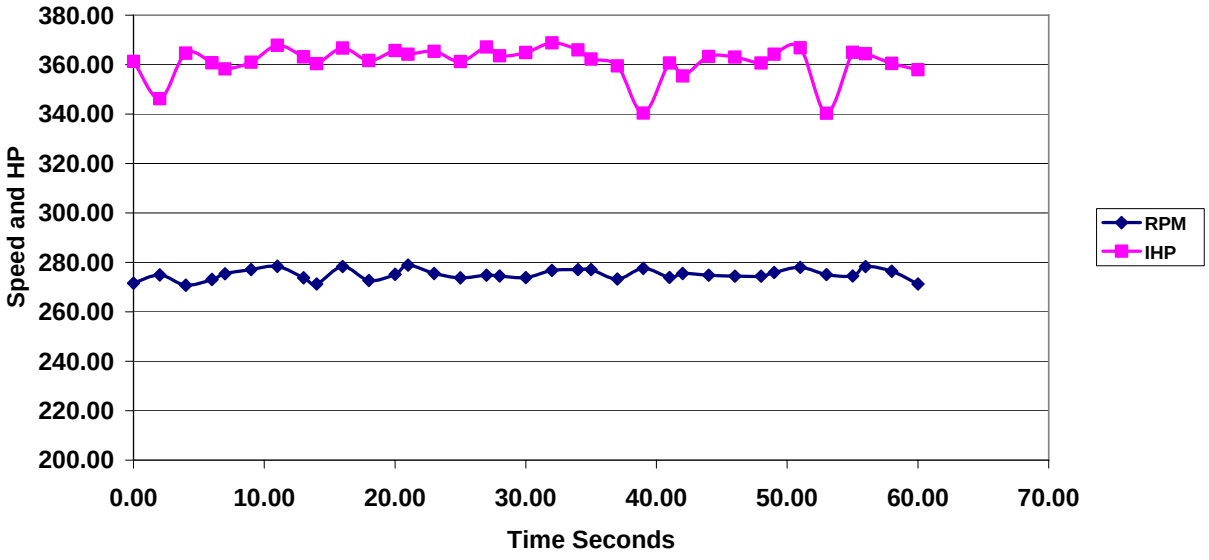

Figure 4-11. Cylinder 3 Speed and HP vs. Time in Seconds; Cylinders 1 and 4 Single-Acting; Clark HBA-6 Unit 4 Compressor Cylinders (Duke Energy's Bedford Station; March 1, 2005)

Figure 4-12 shows a variation of speed and power when Cylinder 1 is tested with all cylinders double-acting. The power variation almost disappears under double-acting conditions, with a maximum range of 7 HP out of 310 (about 2.3%) and no obvious periodicity. The speed variation is also greatly reduced and does not appear to exceed 2 RPM in range (well below 1%).

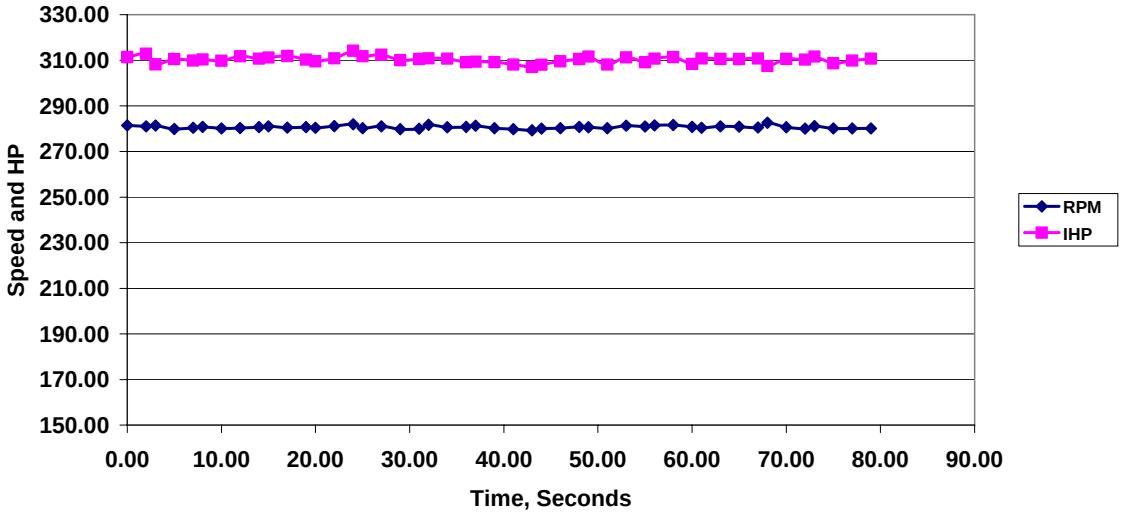

Figure 4-12. Cylinder 1 Speed and HP vs. Time in Seconds; All Cylinders Double-Acting; Clark HBA-6 Unit 4 Compressor Cylinders (Duke Energy's Bedford Station; March 1, 2005)

4.6 VARIATION OF NOZZLE PULSATIONS WITH TIME

Figure 4-13 shows the variation with time of suction and discharge nozzle pulsation peak-to-peak amplitudes for Cylinder 1 when Cylinders 1 and 3 are single-acting. There is a clear modulation in range for the pulsations, and the modulation in range has similar periodicity to the variation of power observed in Figure 4-10. The pulsations have a maximum amplitude approaching 8% of line pressure and average about 5% of line pressure. Interestingly, the variations in suction and discharge nozzle pulsation amplitudes are in phase with each other—suggesting an interaction through the cylinder. The range of variation of the suction nozzle pulsation amplitudes is notably less than the range for discharge pulsation amplitudes.

Figure 4-14 shows that similar characteristics are exhibited by the peak-to-peak amplitudes of pulsations in the suction and discharge nozzles of Cylinder 3 when Cylinders 1 and 4 are single-acting, even when this cylinder itself is double-acting.

When all cylinders are double-acting, Figure 4-15 shows the range of Cylinder 1 modulation in suction and discharge nozzle pulsation amplitudes substantially decreases, and the peak nozzle pulsation amplitude for Cylinder 1 is now about 3%, as opposed to almost 8% under single-acting conditions. Discharge nozzle pulsations are now slightly higher than suction nozzle pulsations, although both are much lower.

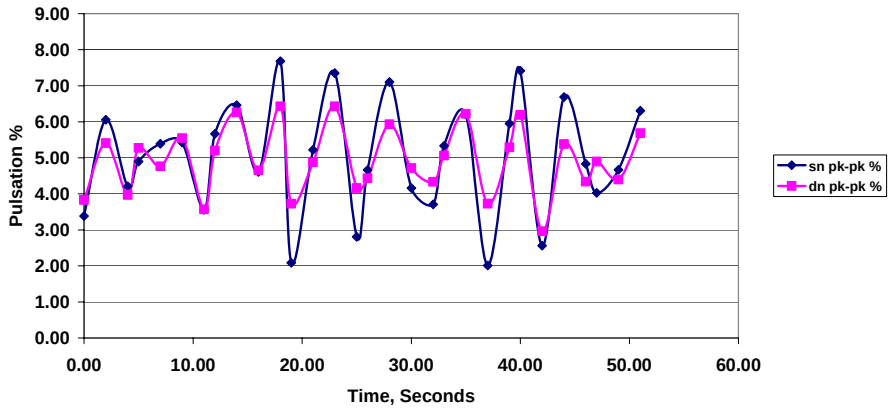

Figure 4-13. Cylinder 1 Suction and Discharge Nozzle Pulsations vs. Time in Seconds; Cylinders 1 and 4 Single-Acting; Clark HBA-6 Unit 4 Compressor Cylinders (Duke Energy's Bedford Station; March 1, 2005)

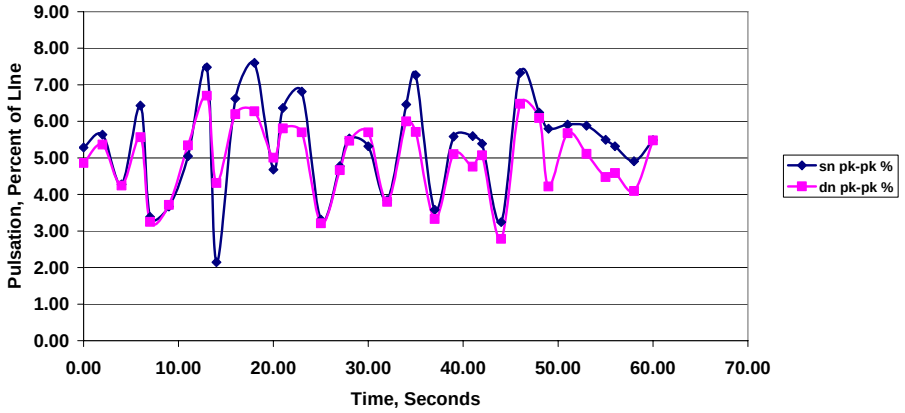

Figure 4-14. Cylinder 3 Suction and Discharge Nozzle Pulsations vs. Time in Seconds; Cylinders 1 and 4 Single-Acting; Clark HBA-6 Unit 4 Compressor Cylinders (Duke Energy's Bedford Station; March 1, 2005)

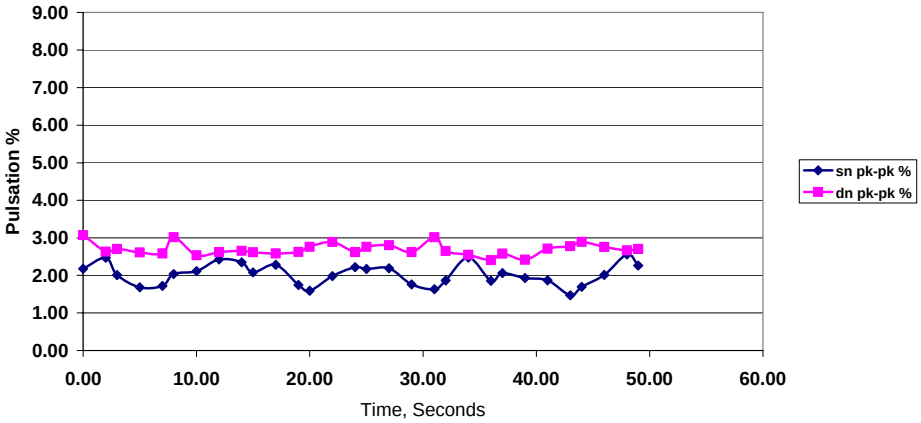

Figure 4-15. Cylinder 1 Suction and Discharge Nozzle Pulsations vs. Time; All Cylinders Double-Acting; Clark HBA-6 Unit 4 Compressor Cylinders (Duke Energy's Bedford Station; March 1, 2005)

4.7 AVERAGED POWER UNDER SINGLE-ACTING CONDITIONS

Figure 4-16 shows the averaged horsepower and its standard deviation estimate for the four compressor cylinders under single-acting conditions in Cylinders 1 and 4. This data results from averaging the horsepower values calculated from individual pressure records obtained at about 2-second intervals (as opposed to a single power calculation from a cycle averaged pressure record). As would be expected, the two single-acting cylinders (1 and 4) show power values, which are less than half the power values for the two double-acting cylinders. The standard deviations in power are the largest for one of the single-acting cylinders (Cylinder 4), but the next highest standard deviation comes from Cylinder 3 (which was double-acting during the tests). The standard deviations range from 1.7% to 5% of the averaged horsepower values in Figure 4-16.

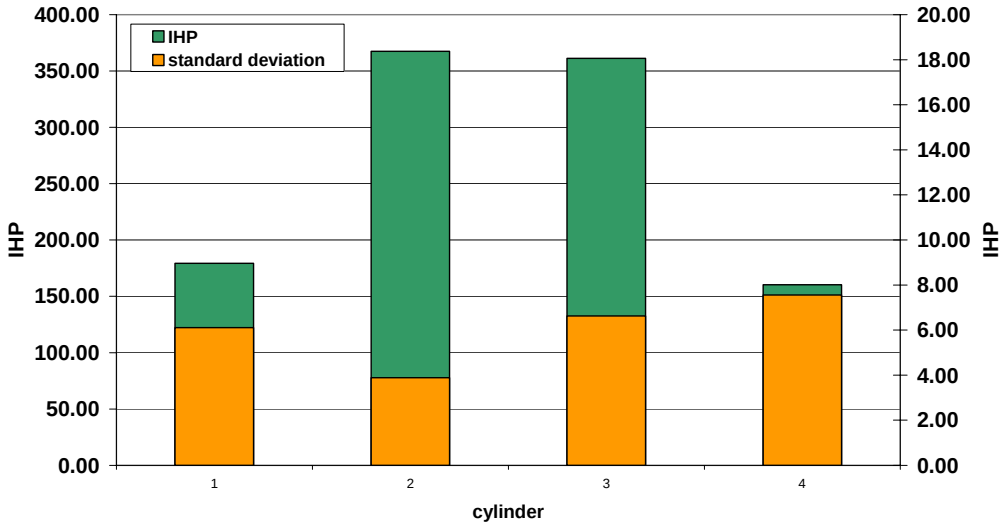

Figure 4-16. Indicated HP – Value and Standard Deviation by Compressor Cylinder with Cylinders 1 and 4 Single-Acting; Clark HBA-6 Unit 4 (Duke Energy's Bedford Station; March 1, 2005)

4.8 COMPARISON OF SINGLE- AND DOUBLE-ACTING POWER AND ITS DEVIATION

Figure 4-17 compares indicated horsepower for each cylinder under single- and double-acting conditions. As Figure 4-6 has shown, the pressure ratio across the unit was substantially lower for the fully double-acting tests. As an intended result, which allowed double-acting operation, the power of all cylinders is about 50 HP below the power of Cylinders 2 and 3 under single-acting conditions. All cylinders are close to equally loaded under double-acting conditions.

Figure 4-18 shows that the standard deviation in power drops substantially when all cylinders are double-acting. The highest standard deviation for any cylinder of 7.5 HP, when single-acting, is reduced to a maximum of 2 HP under double-acting conditions. This is consistent with the reduction in the range of variation seen for Cylinder 1 between Figure 4-10 and Figure 4-12. The sum of single-acting deviations is 24 HP (out of 1,050 HP total for the unit); the sum of double-acting deviations is 6 HP (out of 1,200 HP for the unit).

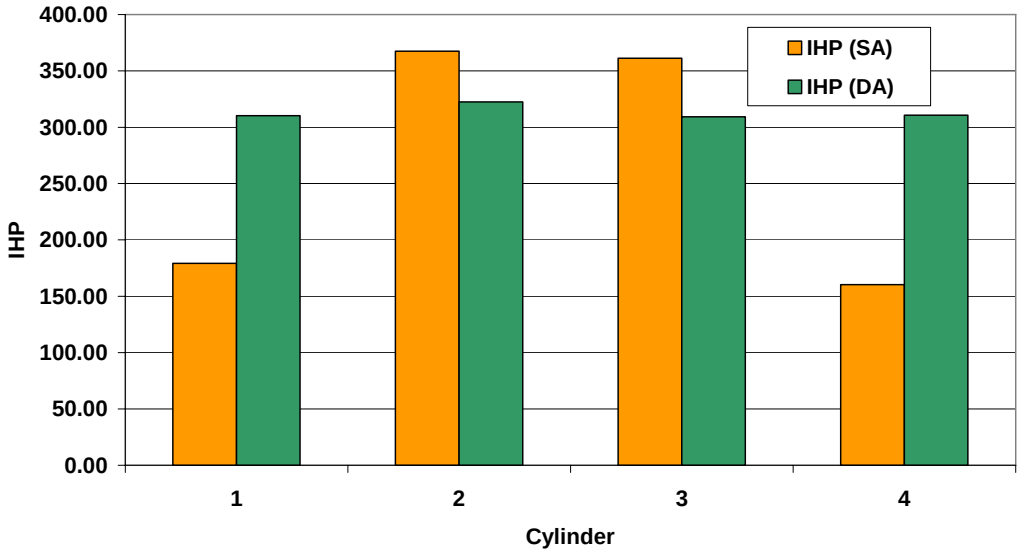

Figure 4-17. Indicated Compressor HP for Each Cylinder – Comparison of Single-Acting and Double-Acting Operation; Clark HBA-6 Unit 4 (Duke Energy's Bedford Station; March 1, 2005)

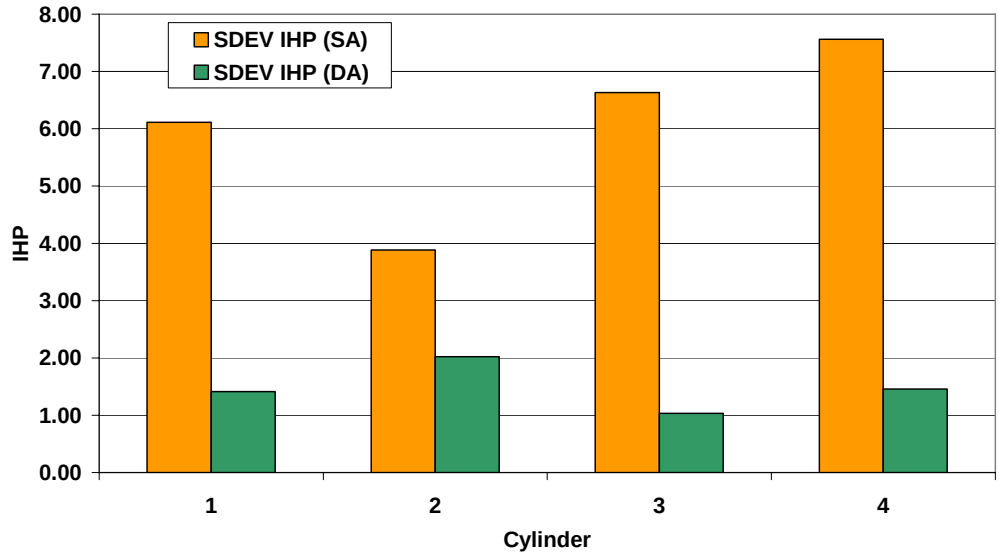

Figure 4-18. Standard Deviation in Indicated Cylinder HP – Comparison of Single-Acting and Double-Acting Operation; Clark HBA-6 Unit 4 (Duke Energy's Bedford Station; March 1, 2005)

Thus, power is much more consistent and more consistently measurable under double-acting conditions.

4.9 COMPARISON OF SINGLE- AND DOUBLE-ACTING PULSATIONS

Figure 4-19 confirms for all cylinders what was observed for Cylinder 1 in Figure 4-13 and Figure 4-15. Average suction nozzle pulsations drop substantially under double-acting conditions. A high pulsation of almost 6% of line pressure under single-acting conditions drops to 2% under double-acting conditions.

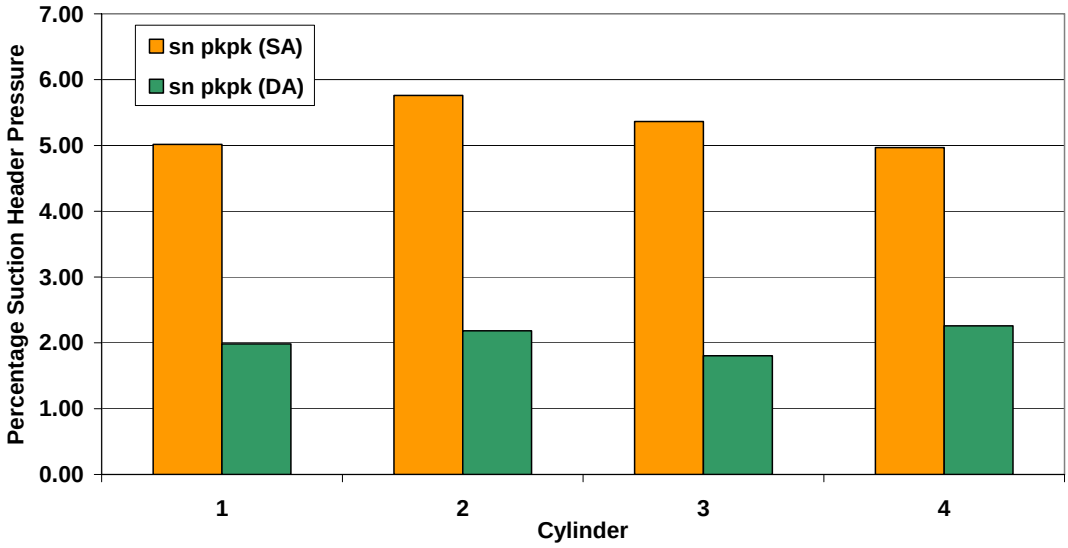

Figure 4-19. Suction Nozzle Pulsation – Comparison of Single-Acting and Double-Acting Operation; Clark HBA-6 Unit 4 (Duke Energy's Bedford Station; March 1, 2005)

Figure 4-20 shows a drop in average discharge nozzle pulsations. The drop is not as dramatic as the drop in average suction nozzle pulsations, but it is distinct.

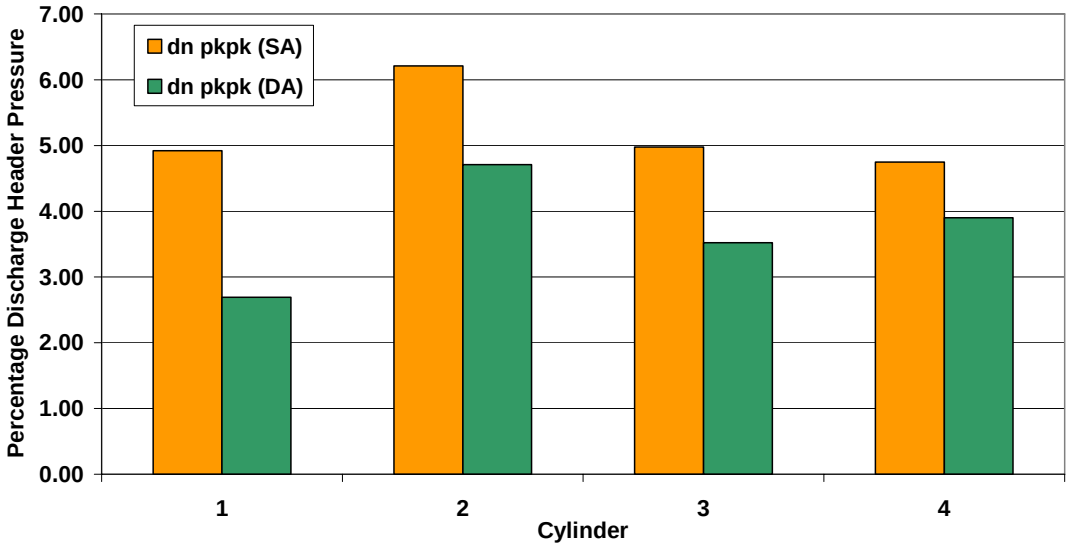

Figure 4-20. Discharge Nozzle Pulsation – Comparison of Single-Acting and Double-Acting Operation; Clark HBA-6 Unit 4 (Duke Energy's Bedford Station; March 1, 2005)

Figure 4-21 and Figure 4-22 show, for both suction nozzle and for discharge nozzle pulsations, a very substantial drop in their standard deviation, indicating a great reduction or elimination of the "beating" phenomenon.

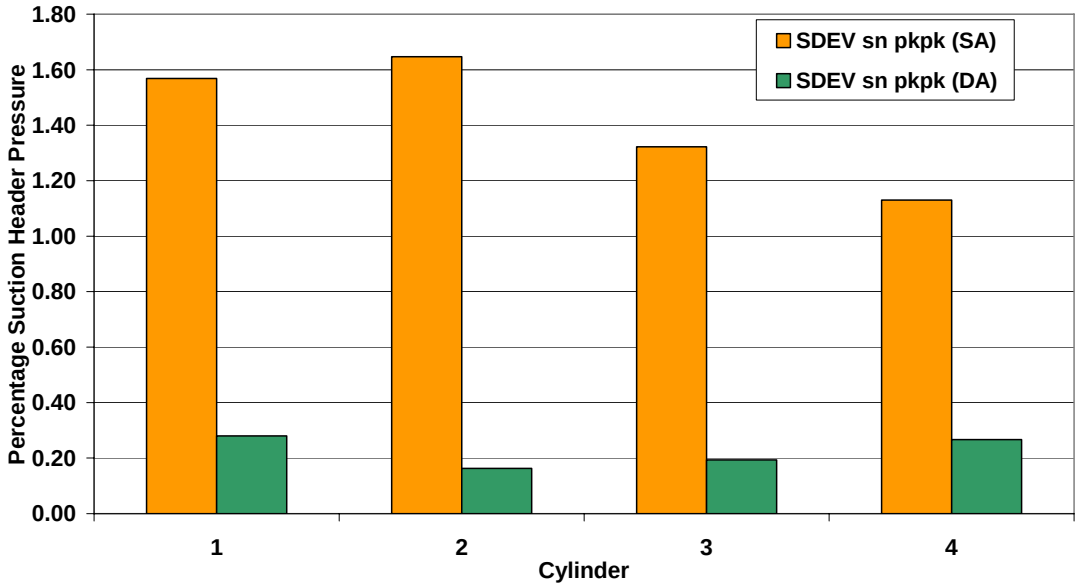

Figure 4-21. Standard Deviation in Suction Nozzle Pulsation – Comparison of Single-Acting and Double-Acting Operation; Clark HBA-6 Unit 4 (Duke Energy's Bedford Station; March 1, 2005)

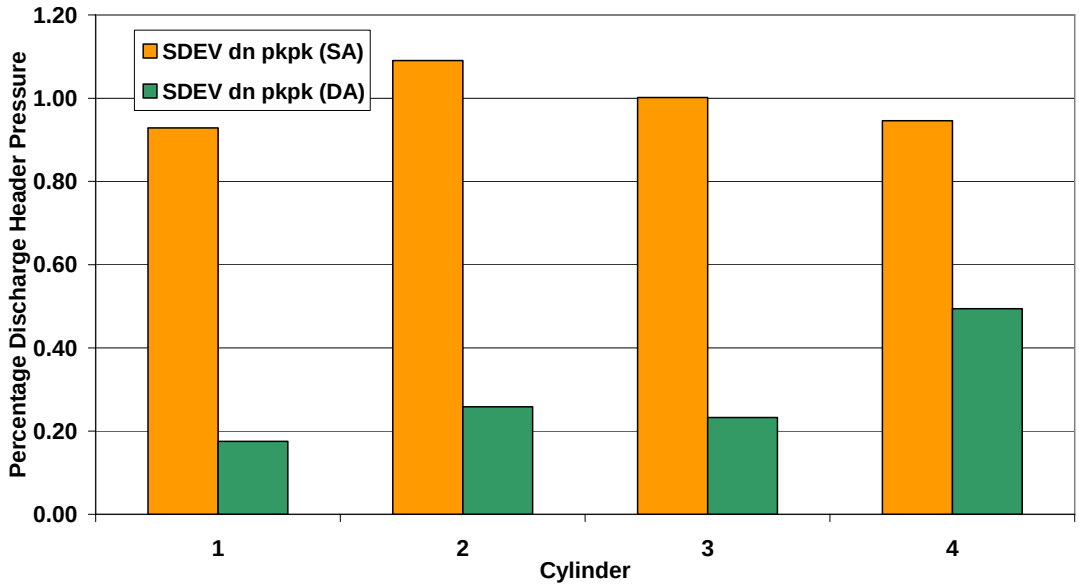

Figure 4-22. Standard Deviation in Discharge Nozzle Pulsation – Comparison of Single-Acting and Double-Acting Operation; Clark HBA-6 Unit 4 (Duke Energy's Bedford Station; March 1, 2005)

Figure 4-23 and Figure 4-24 show that suction (sl) and discharge lateral (dh) pulsations are likewise reduced. Both reduce by about a factor of two in going from single-acting on Cylinders 1 and 4 to double-acting on all cylinders.

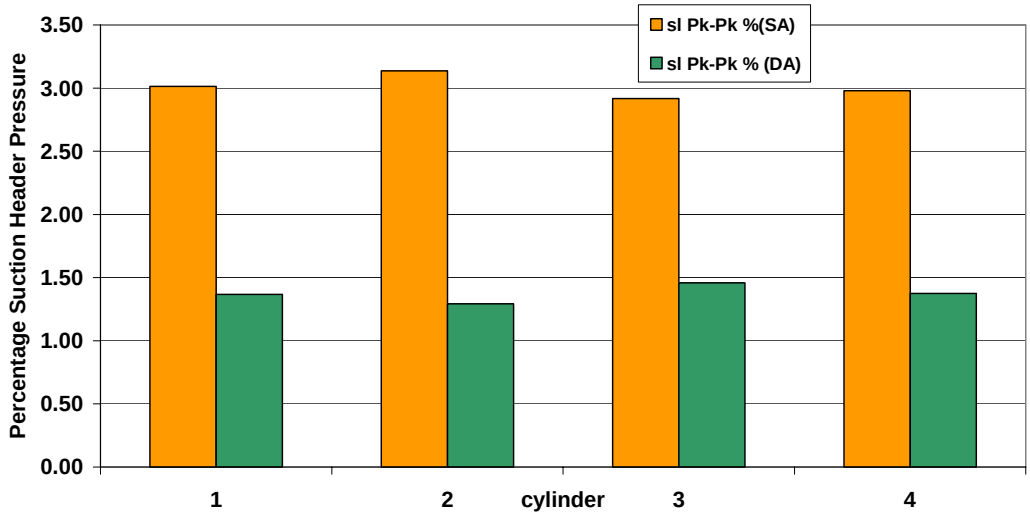

Figure 4-23. Suction Lateral Pulsation – Comparison of Single-Acting and Double-Acting Operation; Clark HBA-6 Unit 4 (Duke Energy's Bedford Station; March 1, 2005)

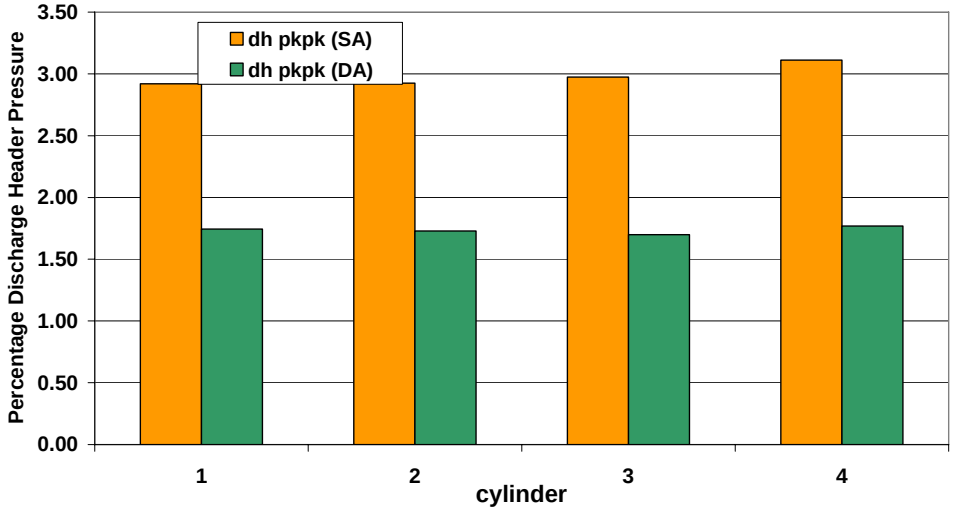

Figure 4-24. Discharge Lateral Pulsation – Comparison of Single-Acting and Double-Acting Operation; Clark HBA-6 Unit 4 (Duke Energy's Bedford Station; March 1, 2005)

4.10 COMPARISON OF COMPRESSOR PERFORMANCE FOR SINGLE- AND DOUBLE-ACTING CONDITIONS

Figure 4-25 compares the Indicated Horsepower per Million Standard Cubic Feet per Day (ICHP/MMSCFD) for the single- and double-acting conditions tested. Clearly, the ICHP/MMSCFD drops significantly between single- and double-acting conditions. However, care must be exercised in interpreting the implied change in compression efficiency because conditions have changed—specifically, the pressure ratio across the compressor, and it is known that ICHP/MMSCFD is a direct function of ratio. These comparisons are presented in Figure 4-25 by cylinder; the comparison will be addressed subsequently for the unit as a whole.

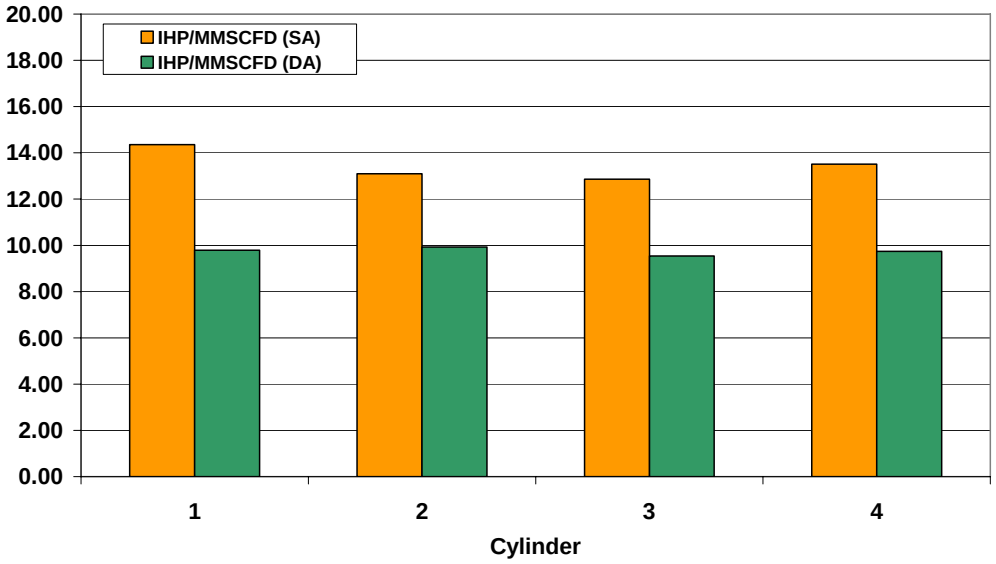

Figure 4-25. Indicated Compressor HP per Million Standard Cubic Feet Per Day (ICHP/MMSCFD) for Each Cylinder – Comparison of Single-Acting and Double-Acting Operation; Clark HBA-6 Unit 4 (Duke Energy's Bedford Station; March 1, 2005)

4.11 UNIT AVERAGE COMPARISONS

Figure 4-26 compares for the unit as whole averaged values for IHP/MMSCFD and pulsations in the nozzles (sn, dn, pk-pk%) and in the lateral lines (sl, dl, pk-pk%). The average pulsations go down typically by a factor of two between single- and double-acting conditions.

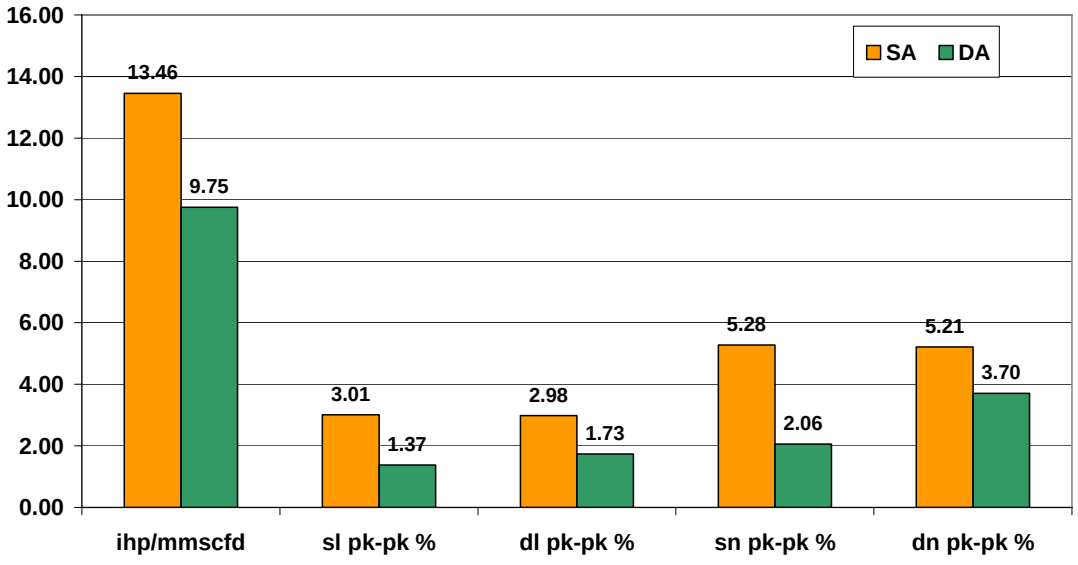

Figure 4-26. Average Performance and Pulsation – Comparison of Single-Acting and Double-Acting Operation for Unit; Clark HBA-6 Unit 4 (Duke Energy's Bedford Station; March 1, 2005)

The average ICHP/MMSCFD for the unit goes down from 13.46 to 9.75. Expressed as the ratio of single-acting to double-acting for ICHP/MMSCFD, the ratio is 1.38.

4.12 COMPARISON OF UNIT PERFORMANCE CHANGE ACCOUNTING FOR CONDITIONS

If we seek the ratio of ideal ICHP/MMSCFD for the two sets of operating conditions and compare this ratio with the ratio of measured ICHP/MMSCFD, we have a sounder basis for comparing performance under the two conditions.

The GMRC report commonly referred to as TR84-10 provides the following relationship:

Theoretical Gas HP (TGHP) ≈ EVs*RPM*Psuc*((Pdis/Psuc)^(k-1)/k-1), where k is the isentropic coefficient. Table 4-1 presents an evaluation of this relationship with two alternative assumptions, A and B:

A Volumetric Efficiency is the same for single-acting and double-acting conditions
This gives a theoretical ratio of 1.29 for single- to double-acting

B Mass Flow ≈ EVs * RPM * Psuc (which implies density ~ Psuc)
This gives a theoretical ratio of 1.37 for single- to double-acting

Table 4-1. Comparison of Theoretical and Measured HP Ratios for Single- and Double-Acting; Clark HBA-6 Unit 4 (Duke Energy's Bedford Station; March 1, 2005)

	SINGLE-ACTING	DOUBLE-ACTING
Psuc Header (g)	768.4	803
Pdis Header (g)	988	966
Tsuc Header	48.94	50.175
Isentropic K	1.35	1.35
Average RPM	275	280
Pressure Ratio	1.2804	1.1993
(k-1)/k	0.2593	0.2593
Header Pressure Ratio$^{((k-1)/k)-1}$	0.0662	0.0483
A. TGHP Ratio (sa/da)	1.2901 (Assumes Volumetric Efficiency is the same for Single- and Double-Acting Conditions)	
B. TGHP/MMSCFD Ratio (sa/da)	1.3716 (Assumes Mass Flow Varies as EVS * RPM * Psuc)	
Measured IHP/MMSCFD ratio (sa/da)	1.3800	

The measured ratio for single- to double-acting is 1.38.

Thus, for either assumption, the measured ratio of power exceeds the theoretical ratio accounting for differences in conditions—for assumption A by 7.8% and for assumption B by 0.7%.

The thermophysical properties used in this and the next section are based on the BWR equation of state for a gas composition of 95% methane; 3.5% ethane; 1% propane; and 0.5% CO_2. This composition was selected before the specific gas composition was available, but conforms very closely to the composition subsequently obtained.

4.13 COMPARISON OF ISENTROPIC EFFICIENCY FOR SINGLE- AND DOUBLE-ACTING CONDITIONS

Isentropic Efficiency is defined as follows:

$\eta_{isen} = \Delta h_{ideal} / \Delta h_{actual}$

Where:

Δh_{ideal} is calculated as $h(P_d, S = S(P_s, T_s)) - h(P_s, T_s)$

Δh_{actual} is calculated as $h(P_d, T_d) - h(P_s, T_s)$

In addition, these h values are calculated using real gas properties (e.g., BWR) for the relevant mixture, and the calculation of $h(P_d, S = S(P_s, T_s))$ requires iteration until the entropy (S) matches suction entropy.

Table 4-2 implements this calculation. It first finds the discharge temperature at which discharge entropy equals suction entropy. It finds this isentropic discharge temperature for single- and for double-acting conditions. It then calculates efficiency two ways from knowledge of the isentropic discharge temperature—first, as the ratio of ideal to actual temperature rise (which implies an assumption that enthalpy is proportional to temperature), and secondly, as the ratio of ideal to actual enthalpy rise, which is the most rigorous method as defined above.

Table 4-2. Calculation of Isentropic Efficiency for Single- and Double-Acting; Clark HBA-6 Unit 4 (Duke Energy's Bedford Station; March 1, 2005)

HEADER CALCULATIONS (DA MODE)				HEADER CALCULATION (SA MODE)			
Pressure (PSIA)	**Tdis (estimate)**	**Enthalpy**		**Pressure (PSIA)**	**Tdis (estimate)**	**Enthalpy**	
817.7	50.1750	2.1210	Target Entropy	783.1	48.94	2.1380	Target Entropy
980.7	83.6700	2.1320		1002.7	80.00	1.1360	
980.7	76.7500	2.1240		1002.7	75.00	2.1300	
980.7	75.0000	2.1220		1002.7	82.00	2.1380	Tdis (constant E) = 82
980.7	74.0000	2.1200	Tdis (constant E) = 74.5				
Tdis/Tsuc	10.48			Tdis/Tsuc	1.065		
Pdis/Psuc	1.199			Pdis/Psuc	1.280		
LR	0.256			LR	0.255		
k1	1.345			k1	1.342		
T based Efficiency	**91.55%**			T based Efficiency	**89.35%**		
P	**T**	**Enthalpy**		**P**	**T**	**Enthalpy**	
817.7	50.175	213.695		783.1	48.94	216.157	
980.7	74.5	223.557		1002.7	82	229.72	
980.7	76.75	225.015		1002.7	85.94	232.269	
Enthalpy Based Efficiency	**87.12%**			Enthalpy Based Efficiency	**84.18%**		
Ratio of Isentropic Efficiencies	**103.5%**						

Figure 4-27 then presents and compares the four efficiency calculations. The more rigorous method gives 87.12% for double-acting operation and 84.18% for single-acting conditions. The ratio of these two efficiencies is 1.035—that is, the single-acting operation exhibits a 3.5% penalty relative to double-acting operation. For a given flow, this means 3.5% more fuel is burned when single-acting than if the conditions could be achieved with all cylinders double-acting. If the unit is being operated at maximum load, it is losing 3.5% of its capacity to losses under single-acting conditions, which are not present under double-acting conditions.

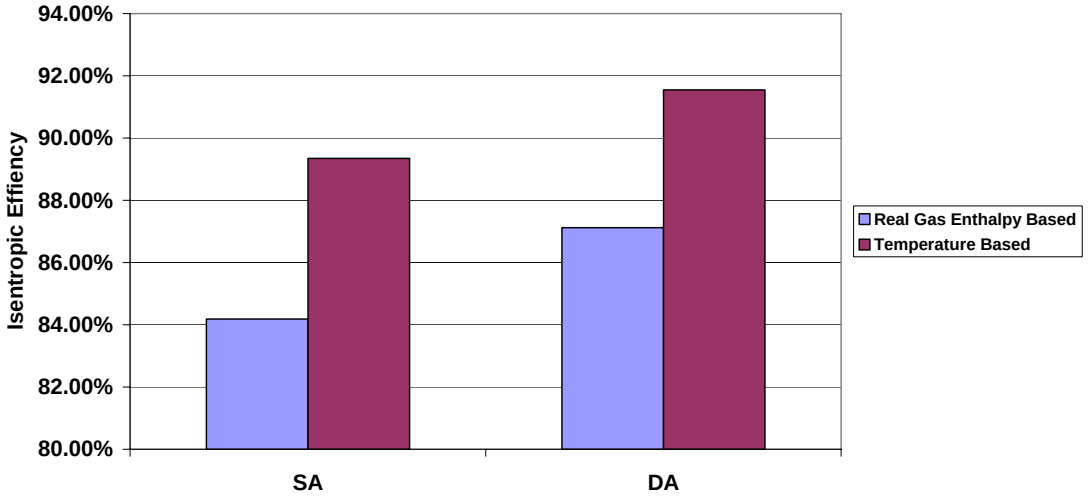

Figure 4-27. Comparison of Isentropic Efficiency for Single- and Double-Acting Operation; Clark HBA-6 Unit 4 (Duke Energy's Bedford Station; March 1, 2005)

4.14 DISTINGUISHING COMPRESSOR LOSSES

To identify when changes to operation or to configuration will be beneficial, it is desirable to be able to distinguish losses attributable to irreversibility during nominally isentropic compression, losses attributable to valve flow resistance, and losses attributable to flow resistance in the attached compressor manifold system and lateral piping. To this end, a prototype methodology has been defined and will be illustrated with a data sample from Unit 4 at Duke Energy's Bedford Station, as follows.

4.14.1 Data Required

The method starts with measured time-varying pressure in the cylinder, the suction and discharge nozzles, and the laterals. This data is acquired with well-calibrated transducers, by a data acquisition system, which triggers sampling at 512 intervals per compressor crankshaft rotation, each cycle starting at the same point of crankshaft rotation. Thirty-two records of 512-point data are acquired and synchronously averaged. The resultant averaged pressure record is corrected for channel resonance distortion (Harris, et al., [4]). Figure 4-28 illustrates a typical pressure (P) versus crank angle (θ) record ("PT card"), which results from this data acquisition process and pre-conditioning. This is for Cylinder 2 during universal double-acting operation. Table 4-3 shows the numerical results of the steps in the calculation process described below, as applied to the head-end (black) curve of Figure 4-28.

Table 4-3. Illustrative Calculation for Distinguishing Losses Attributable to Irreversibility, Valves, and Installation; Double-Acting Cylinder 2 HE; Clark HBA-6 Unit 4 (Duke Energy's Bedford Station; March 1, 2005)

Indicated HE HP	168.41	From measured cylinder data
Valve Loss HE % HP	5.88%	From cylinder data and nozzle data
EV based flow	17.05	From cylinder data
Isentropic Toe IHP	129.2	Computed using isentropic K = 1.324 and toe pressures
Lossless Card Toe HE IHP	131.92	Computed by forcing flat lines on measured cylinder data at Toe pressures
Cylinder Losses (between Toes)	1.62%	Difference associated with non-isentropic cylinder, leaks and so on, should not be charged to install
Cylinder Losses (between Toes)	2.11%	Same as above but expresses as percent of Isentropic Toe IHP
Isentropic Lateral HE HP	143.47	Computed using average measured lateral pressures, measured EV, and isentropic K = 1.344
EV based flow	16.62	Estimated from isentropic card above (slightly different than actual card since pressures are different)
Predicted Cylinder Lateral HP	150.28049	Computed from line 10, corrected for flow and cylinder losses (line 7)
Measured IHP minus valve loses	158.50749	
Estimated Installation Losses (% IHP)	4.89%	Measured valve-less IHP minus Predicted cylinder lateral HP (line 14-line 12)
Total Losses %	12.38%	
Overall Efficiency	87.62%	

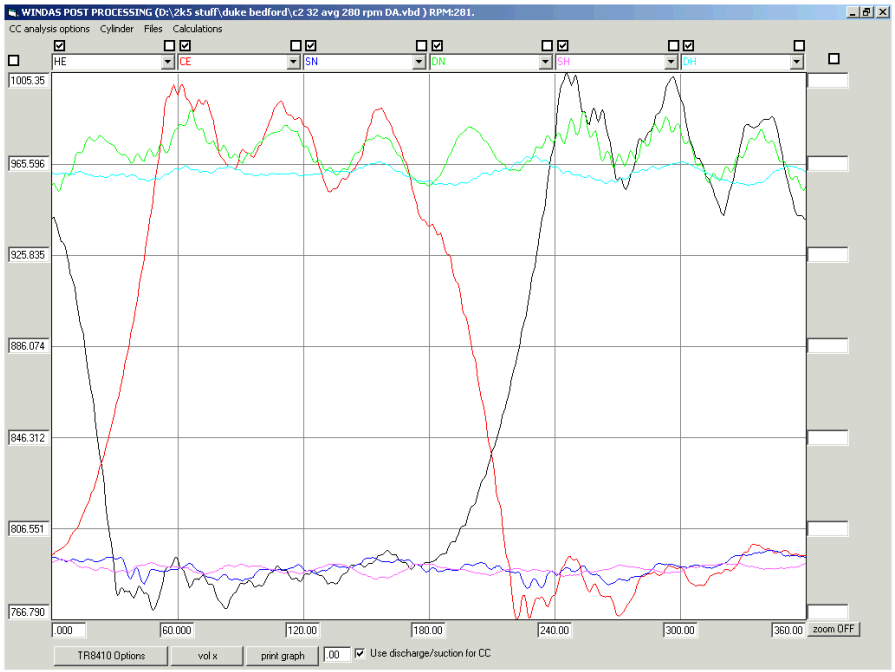

Figure 4-28. Illustrative Channel Corrected Data from Cylinder 2 Under All Double-Acting Operation; Clark HBA-6 Unit 4 (Duke Energy's Bedford Station; March 1, 2005)

4.14.2 Calculation Process

1. Calculate the work done per cycle $\oint PdV$, where V is the instantaneous volume of the cylinder end, calculated as a function of the crank angle based on kinematics of the slider crank mechanism driving the piston. The result is in in.lb/cycle if pressure is PSI and volume is in cubic inches; using the instantaneous rotational speed in rev/sec, calculate the rate of doing work (in.lb/sec) and divide by 6,600 to convert to horsepower. Table 4-3 shows the result is 168.41 HP.

2. From the Cylinder pressure and Nozzle pressure records, calculate the differential work done against valve flow resistance (suction and discharge valves) as a percentage of the work per cycle calculated for the cylinder end in the preceding step. Table 4-3 shows this to be 5.88%.

3. Calculate ideal flow as $\rho_s * EV_s * V_{swept} * RPS$, i.e., the product of density, volumetric efficiency, swept volume, and the speed in revolutions per second. Density comes from a thermophysical property calculation for the flowing gas, EV_s is the difference in swept volume between bottom dead center volume and volume at BDC toe pressure on the re-expansion line. (See next step for more definition of toe pressures). Table 4-3 shows this flow to be 17.05 MMSCFD.

4. Estimate isentropic work between the toe pressures. The toe pressures occur at top dead center (TDC – minimum volume) and bottom dead center (BDC – maximum volume) for the cylinder end in question. The isentropic work is based on a similar calculation of work done per cycle as performed on the actual measured PT card, but the card in question is horizontally flattened at the suction and discharge toe values (illustrated in Figure 4-29), and pressure varies between the pressures by following an isentropic relationship between pressure and volume (PV^k=constant), where k = ln(P1/P2)/ln(V2/V1) and 1 and 2 refer to bottom and top dead center, respectively. Convert to horsepower. Table 4-3 shows the result to be 129.2 HP.

5. Calculate work done from the "valve lossless" measured card, i.e., with the measured card flattened at the same suction and discharge toe pressures as the isentropic card described in the preceding step, but with pressure following the measured variation with volume in between these maximum and minimum pressures. Convert to horsepower. Table 4-3 shows the result to be 131.92 HP.

6. Calculate the difference between the valve lossless measured card HP and the isentropic HP; this is interpreted as the irreversibility loss from the compression and re-expansion segments of the PT card. Table 4-3 shows that, expressed as a percentage of the measured card HP, this is 1.62%, and expressed as a percentage of the isentropic power, it is 2.11%.

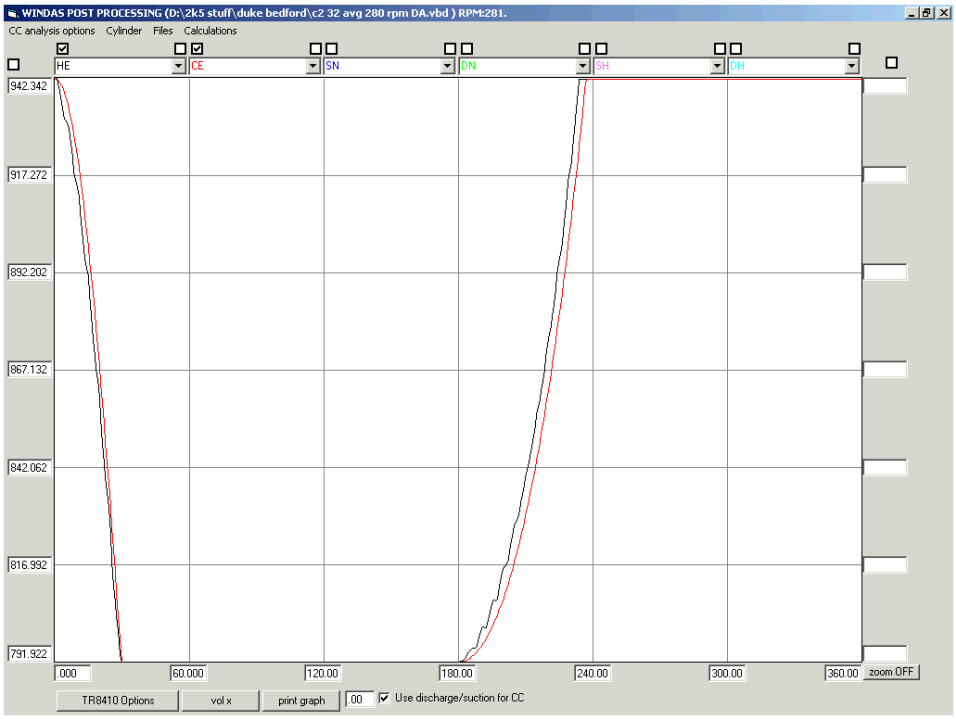

Figure 4-29. Toe Isentropic Card and Flattened Measured Card for Cylinder 2 Under All Double-Acting Operation; Clark HBA-6 Unit 4 (Duke Energy's Bedford Station; March 1, 2005)

7. Calculate isentropic power and flow for the same cylinder end working between the averaged lateral line pressures. Figure 4-30 illustrates this isentropic lateral card, including the horizontally flattened sections at the average lateral suction and discharge pressures. Table 4-3 shows this power to be 143.47 HP.

8. Apply two corrections or adjustments to this isentropic lateral power; increase it by the percentage of irreversibility loss determined from the cylinder card as described above and by the ratio of EV based flow for the cylinder card to EV based flow for the isentropic lateral card. Table 4-3 shows the result of these corrections is 150.28 HP.

9. Calculate the installation loss as the difference between the measured power with valve losses subtracted and the lateral isentropic power. Table 4-3 shows the result to be 4.89% of the measured power. Table 4-3 further shows that the total of Valve + Installation + Irreversibility loss is 12.38% of the measured power. Expressed as efficiency, this yields 87.62% (close to the isentropic efficiency of 87.12 % given in Table 4-2).

4.15 DISCUSSION OF RESULTS AND ILLUSTRATIONS

The above methodology would be applied to each end of the compressor and used to assess the opportunity for loss reduction by installation changes. It will be applied, to the extent possible, to data obtained from survey site tests. It will also be applied to the data obtained from more detailed testing at the selected site.

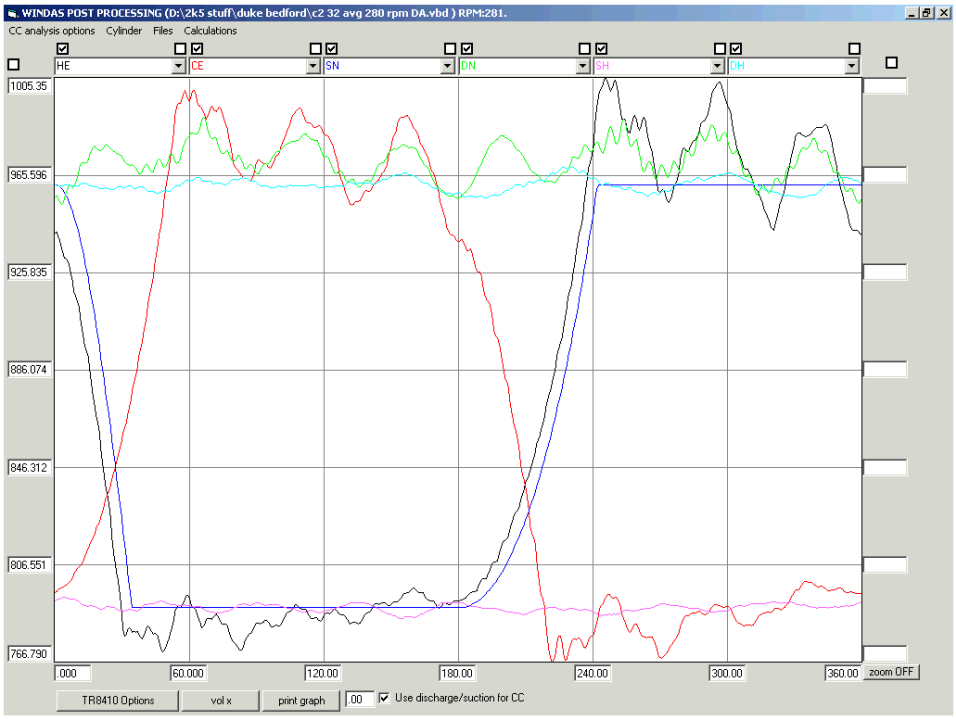

Figure 4-30. Isentropic Lateral Card for Cylinder 2 Under All Double-Acting Operation; Clark HBA-6 Unit 4 (Duke Energy's Bedford Station; March 1, 2005)

The illustration shows close to an even split between valve and installation losses for the head-end of Cylinder 2 under double-acting conditions.

The application of this methodology can encounter difficulties if the data is unsteady—as for single-acting conditions, or if these are high nozzle resonances. Some of the nozzles on the HBA units at the Duke Energy Bedford Station, including the unit tested (Unit 4) are longer than others and as a result have more pronounced nozzle resonances.

Table 4-4 shows further analysis of the double-acting data using this methodology, and represents the ends, which could be readily analyzed in this way under the conditions of unsteadiness and nozzle resonance amplitude. From the data in this table, the valve losses are in the range of 5% to 7%, and installation losses are about 5%. The targets of opportunity for this and the other units at this station include the installation losses and the difference in isentropic efficiency (~3.5% difference of the higher double-acting efficiency relative to the lower single-acting efficiency). Reduction of losses will reduce fuel consumption for a given amount of useful compression work and increase capacity at a set engine horsepower limit.

One or more additional survey site tests will be undertaken early in the second quarter of 2005, and an evaluation performed based on data obtained as to plans for further testing and potential modifications in operation and installation.

Table 4-4. Application of Loss Distinguishing Methodology Under Double-Acting Conditions; Clark HBA-6 Unit 4 (Duke Energy's Bedford Station; March 1, 2005)

	C4HE	C1HE	C2HE	C2CE
Indicated HP	161.9	162.91	168.41	153
Valve Loss	7.43	7.68	5.88	5.67
EV Based Flow	16.72	16.35	17.05	15.00
Isentropic Toe IHP	136.6	139.5	129.2	112
Lossless Card Toe HE IHP	136.7	140.5	131.92	114.35
Cylinder Losses (between Toes)	0.06%	0.61%	1.62%	1.54%
Cylinder Losses (between Toes)	0.07%	0.72%	2.11%	2.10%
Isentropic Lateral HP	139.55	137.26	143.47	130
EV Based Flow	15.85	15.79	16.62	14.659
Predicted Cylinder Lateral HP	147.32	143.15	150.28	135.82
Measured HP Minus Valve Losses	149.87	150.40	158.51	144.32
Estimated Installation Losses (% IHP)	1.58%	4.45%	4.89%	5.56%
Total Losses %	9.07%	12.75%	12.38%	12.77%
Overall Efficiency	90.93%	87.25%	87.62%	87.23%

4.16 RESULTS AND DISCUSSION FOR AIR BALANCE TASKS

The work completed on the Air Balance tasks this quarter include the following:

- GMVH engine has been reassembled after teardown to conduct a detailed geometric analysis and flow testing of select cylinders. The turbocharger is still at Cooper Compression facilities awaiting mapping, thus the GMVH is not currently operational.
- Data from the geometric analysis and flow bench testing was analyzed and incorporated into the simulation model. The dimensional variation was documented in the previous quarterly report.
- With the new information derived from engine measurements, especially the large plenum in the base, the simulation model was finally validated to baseline test data. After validation was completed successfully, development of conceptual designs was begun. Simulation of the conceptual designs and optimization of the geometry is in progress.
- A TOC review meeting is planned at SwRI for May 4, 2005. A presentation will be given to the GMRC PSC at this same time.

4.16.1 GMVH Engine Testing

Prior engine testing involved operation in both open chamber and pre-chamber configurations. The engine tested over engine speeds of 231, 264, 297, and 330 RPM. Engine load was also varied from 70, 85, 90, and 100 of rated. Within this map of engine speed and load, the air/fuel ratio and spark timing was varied. In analyzing the data, the spread of compression pressures was seen to remain very consistent regardless of the operating condition.

This consistency is shown in Figure 4-31, where the pressure at 20 degrees before top dead center (TDC) for all cylinders at all operating conditions tested is plotted versus air manifold pressure.

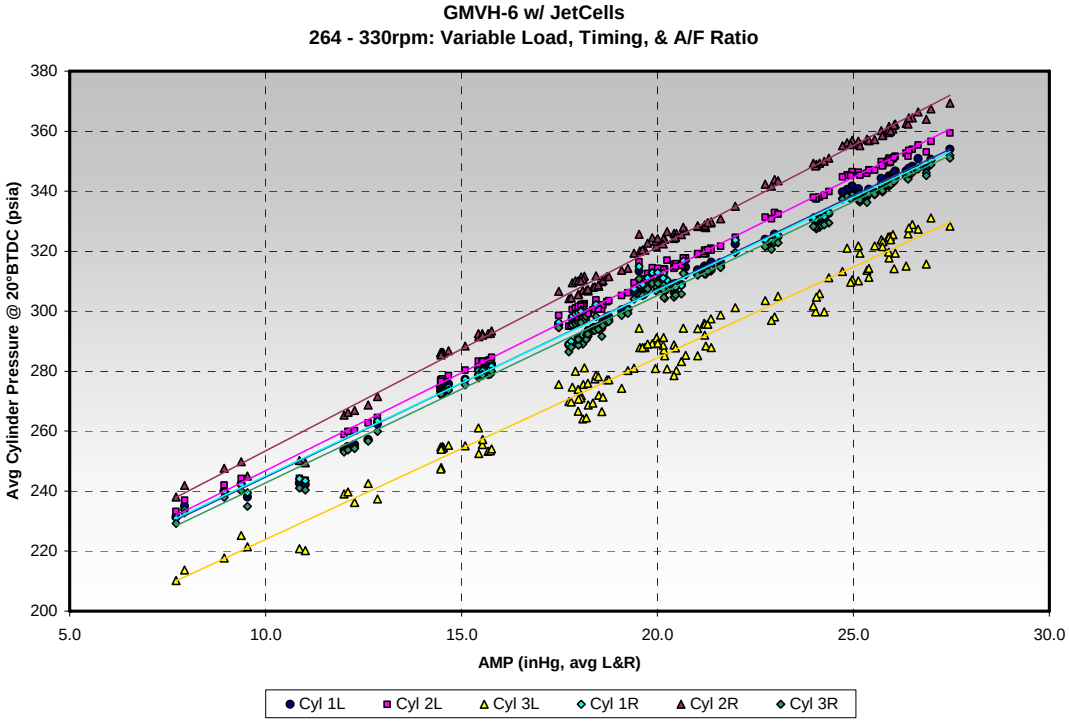

Figure 4-31. Comparison of Cylinder-to-Cylinder Compression Pressure at All Operating Conditions

In the engine simulation subtask, a significant amount of work has been invested in creating a geometric model and characteristics of combustion and turbocharger for the GMVH-6 engine. The baseline test data has been analyzed for characterizing the combustion and engine performance. Data provided by Cooper on the turbocharger and measurements on the test engine were analyzed to create detailed maps of compressor and turbine performance. Drawings and external geometric measurements on the test engine were compiled to model the complex geometry of manifolds, ports, and cylinders.

Several iterations of the software have been compiled to address the specifics of the GMVH engine. Prior simulations have predicted mass airflow closely, but did not accurately predict the amplitude and phasing of pulsations in the inlet and exhaust manifolds. It was believed that the inaccurate manifold dynamic predictions were due to the use of inaccurate discharge coefficients and inaccurate representations of the complicated cylinder plenum geometry that could not be measured externally. In addition, cylinder drawings provided by Cooper showed an allowable casting variation for the exhaust ports, as depicted in Figure 4-32, that gave increased concern of component variability contributing more to air imbalance than originally believed. Thus, it was decided to initiate the geometric analysis and conduct flow testing of select cylinders to resolve uncertainty.

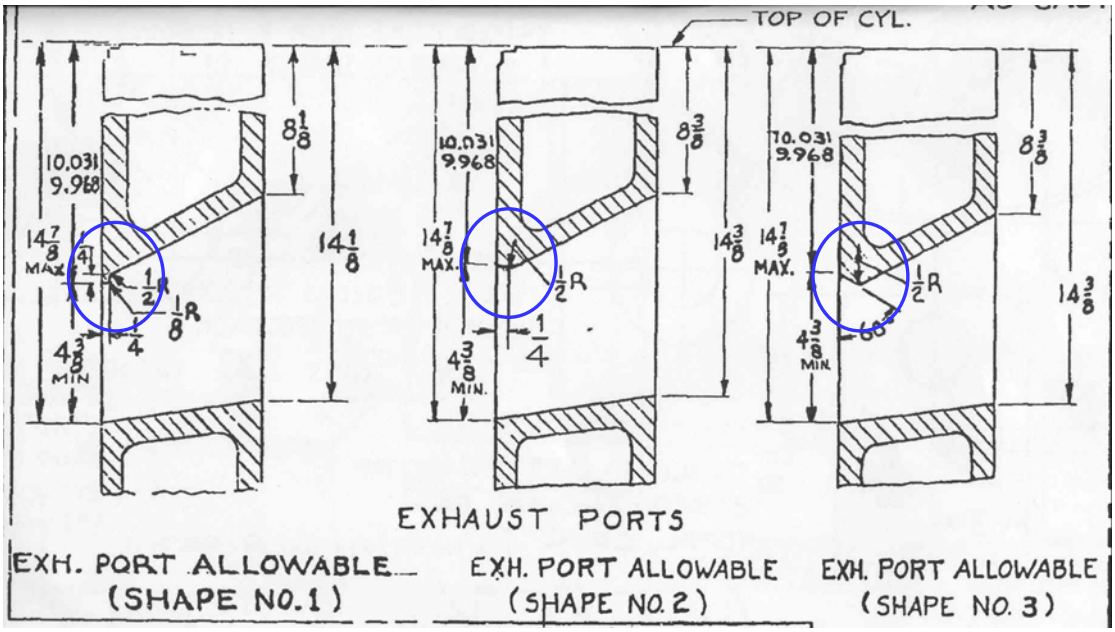

Figure 4-32. Allowable Exhaust Port Geometry

The test engine was disassembled and a geometric analysis conducted. The geometric analysis involved many detailed measurements on all cylinders to quantify the variation cylinder-to-cylinder in compression ratio, inlet and exhaust port timing, and inlet and exhaust port geometry. A list of the static measurements was provided in Table 2-2. From these measurements, several parameters were calculated. There were also three critical discoveries made after the engine had been disassembled. These discoveries were as follows:

1. The cylinder inlet plenum volume was significantly larger than estimated from drawings.
2. A very large plenum in the engine base was connected to each cylinder's intake. This base plenum was not thought to be connected to the intake system on this engine and, therefore, had not been incorporated into the simulation model.
3. Cylinder 1R had the exhaust port shape No. 1, as depicted in Figure 4-32, and the other cylinders had the No. 3 allowable shape. Cylinder 1R had a casting number of GMVG-9-A, and the remaining cylinders had a casting number of GMVA-2-E.

The base plenum was originally the inlet air path when an earlier version of this engine was piston scavenged. It was thought that the base plenum was sealed off from the intake system through blocking gaskets. The size and shape of this volume was also unknown during initial modeling of the GMVH engine. After discovering that the base plenum had been connected, base drawings were requested from Cooper, and additional measurements were made on the engine. The discovery of the base plenum being connected to the inlet system was a very important finding, as accurate simulation would have never been achieved without this feature being incorporated into the model. A simplified CAD model was then generated to calculate the air volume and allow for visual investigation on the proper method to simulate the flow paths. The base plenum volume was estimated at 65,106 in^3 (1,067 L). The CAD representation is depicted in Figure 4-33.

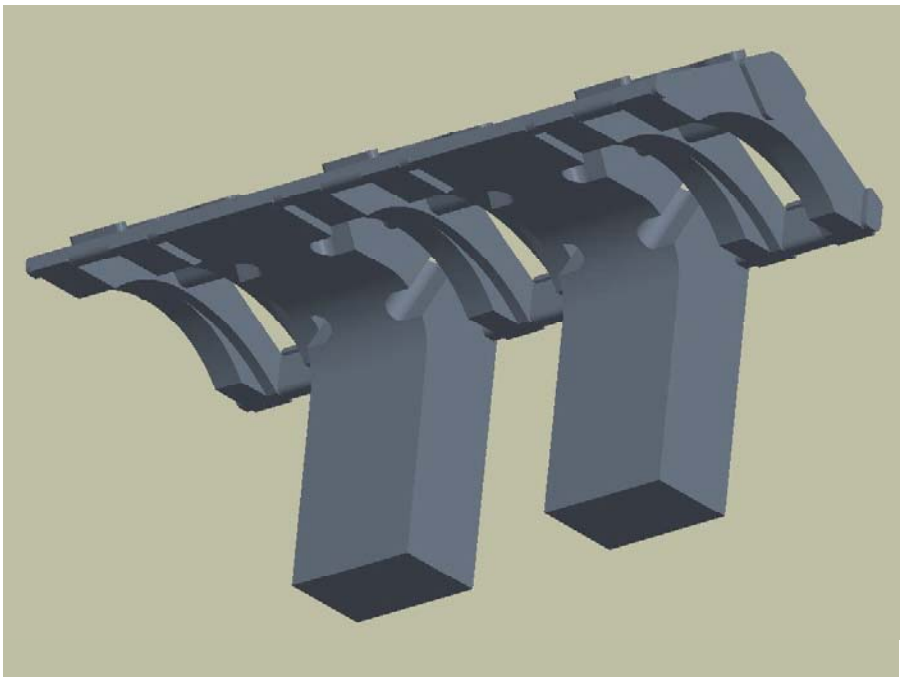

Figure 4-33. CAD Model of Simplified Base Plenum

Geometric data presented in the previous quarterly report showed some variation in compression ratio and port timings between cylinders. At the time, the magnitude of the variations was felt to be within nominal specifications, and it would not be significant to contribute to the variation seen in cylinder pressure data. Flow bench test results also showed variations, but again the magnitude was not felt sufficient to cause the cylinder pressure variations. After extensive simulation efforts, it is now suspected the sum of these variations could be contributing to the variations in compression pressure and, therefore, air balance. During reassembly of the engine, Cylinder 1R was replaced with a similar casting, and Cylinders 1L and 3L were swapped. The effects of cylinder variation will then be tested as soon as the GMVH engine is operational.

4.16.2 GMVH Engine Simulation

The results from the geometric analysis and flow bench testing were incorporated into a revised engine model that now more accurately simulates the GMVH-6 engine. Initial simulations performed with the revised geometry still showed some deviation from baseline test data, although the frequency and amplitude of pulsations was predicted much more accurately. Figure 4-34 shows a comparison of the measured and predicted cylinder pressure from Cylinder 1L from the initial simulations with revised geometry. After significant re-tuning of the model, particularly the turbocharger model, the engine model now accurately captures the deviations between these cylinders. The final validation is shown in Figure 4-35 and Figure 4-36. The comparison of measured and simulated cylinder pressure from Cylinder 1L from the final validated model is depicted in Figure 4-35. Comparisons of measured and simulated inlet and exhaust manifold pressures are depicted in Figure 4-36. An excellent match can be seen in these figures, and confidence in the model is sufficient to begin the conceptual design process.

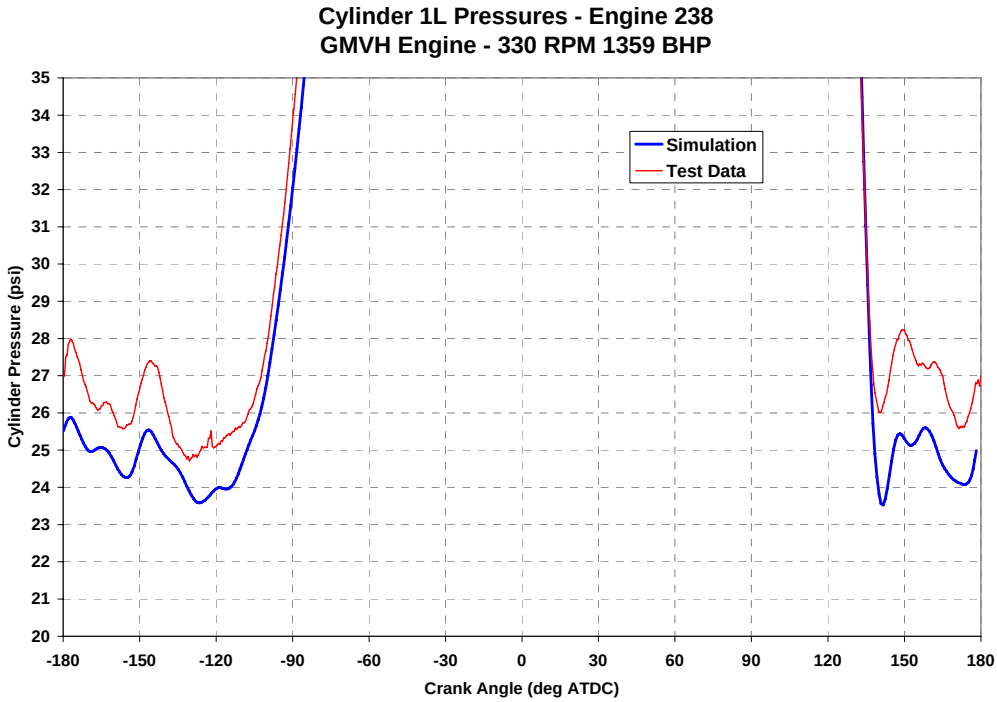

Figure 4-34. Cylinder 1L Measured and Simulated Pressure – Initial Baseline Simulation with Revised Geometry

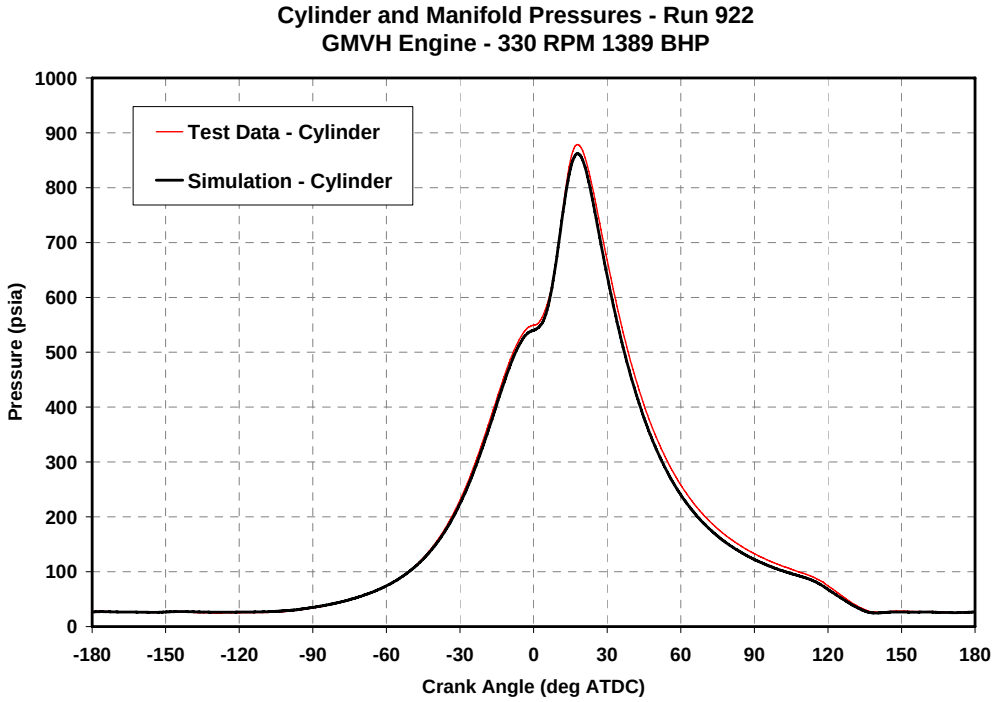

Figure 4-35. Cylinder 1L Measured and Simulated Pressure – Final Baseline Simulation with Revised Geometry

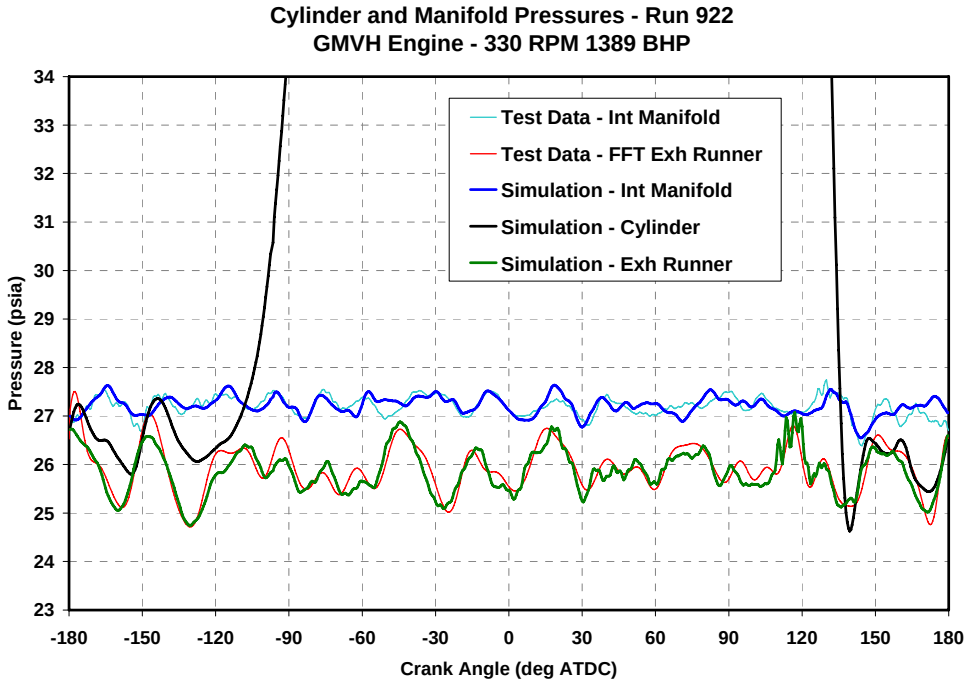

Figure 4-36. Cylinder 1L Measured and Simulated Manifold Pressures – Final Baseline Simulation with Revised Geometry

Achieving a validated model is a significant milestone. The next steps with the model are to investigate the effects on cylinder-to-cylinder air balance from various manifold designs and also the variation in compression ratio, port timing, and port flow that was been documented previously. The manifold design process began with the exhaust side. This was done due to the perceived lack of benefit from re-designing the intake manifold with the base plenum active. However, further investigations have led to the development of one concept that involves both the exhaust and intake manifolds. The following manifold concepts have been developed:

- *Tuned exhaust manifold using individual expansion chambers* – This concept involves the use of individual expansion chambers designed similar to small two-stroke engines. The expansion chamber is designed to reflect a pulse that returns to the cylinder just prior to exhaust port closure to increase the trapped mass of fresh air. The potential benefits of this design are improved trapping efficiency, increased air mass (potential for leaner air/fuel ratios), and increased power. The disadvantages of this design are that each cylinder runner is very long, which could lead to a very expensive design and create packaging issues. Another disadvantage is that this design is very sensitive to engine speed and exhaust temperature, which would create a narrow band of operating conditions where performance is optimized.
- *Tuned exhaust manifold using cylinder pairing* – This concept is similar to the previous in that a pulse is utilized to "pack" the cylinder near port closure to increase trapped mass. This concept differs in that select cylinders are paired and the pulse from one cylinder is used to affect the other cylinder. The performance advantages are similar to the expansion chamber concept. The cost and packaging

issues are somewhat improved but still likely to be a very expensive option. There is also concern that the concept will become more cumbersome with increased number of cylinders. Cylinder phasing, or timing, is critical to the design to achieve proper pulse timing. Therefore, the concept may work well for a six-cylinder engine but not as well for a ten-cylinder engine. These issues are being investigated.

- *Tuned manifold using multiple cylinder connection* – This concept is an extension of the cylinder pairing and involves the coupling of at least three cylinders. This coupling of multiple cylinders would be necessary if the phasing is such that pairing cannot be practically accomplished to achieve the desired pulse timing. Again, potential performance benefits are similar to prior tuned manifold concepts. Packing and cost may improve somewhat with this type design but is still a costly alternative and would require extensive design efforts (as with the previous) to achieve the life span required for these engines.

- *Exhaust manifold retrofit with Side Branch Absorbers (SBA)* – This concept deviates from a tuned manifold concept and seeks to normalize and mitigate pulsations in the exhaust. For air balancing, one method is to develop a concept that creates similar breathing of each cylinder. This SBA concept is expected to dampen a certain frequency of pulsations that are seen in some cylinders but not in others and thought to affect the breathing differently. The SBA is a retrofit of the existing manifold design and, therefore, should be very cost effective. While the potential performance benefit is not as great as with the tuned manifold concepts, balancing the cylinders will be beneficial in terms of performance and emissions. This concept will also be more robust in its benefits across the operating range, and may provide increased performance benefit at off-rated conditions than a specifically tuned manifold.

- *Intake and Exhaust manifold retrofits with SBA* – This concept is an extension of the Exhaust SBA design, adding SBAs to the intake manifolds to allow the base plenum to be disconnected. As mentioned previously, the base plenum has shown in simulation to be creating an elevated temperature of the air mass entering the cylinders. Capping this plenum with gaskets will allow significantly cooler air to enter the cylinders, which will lead to increased mass airflow due to a denser charge. A cooler, denser charge has many performance benefits. Increased trapped mass could lead to leaner operation for reduced NO_x emissions, and the cooler initial temperature provides potential detonation mitigation. This concept would require the cylinder to be removed and the plenum blocked off, causing increased cost of installation. However, it is currently projected that the costs will be significantly less than any of the tuned exhaust manifold concepts. The current thinking is that this concept has the best potential for an optimal cost-benefit ratio.

In addition to the manifold concepts listed above, simulation efforts will also be directed toward potential low cost features for addressing cylinder geometric variations. It has been envisioned that easily installed and replaceable orifice plates can be installed between the intake manifold runners and the cylinders to balance airflow due to port flow variations. This orifice or baffle approach would only be applicable to the intake and exhaust manifold SBA concept due to the removal of base plenum effects. With the base plenum active, the only means to affect flow

on a per cylinder basis is to apply the devices to the exhaust runner. Application to the exhaust side would create problems in terms of integrity and installation.

Design and simulation of the concepts listed above is currently in progress. It is anticipated that the conclusion of this task will occur in the next month. Afterwards, the detailed design task will begin with the chosen conceptual design. The detailed design task will focus on the application to the GMVH-6 laboratory engine.

5. CONCLUSIONS

Based on the data presented in Section 4, the following conclusions can be drawn:

1. The survey site visit process can provide significant, useful data.
2. This data can guide evaluation of opportunities for reduction in installation losses by changes in installation or operation.
3. The unit tested shows distinct unsteadiness in operation with two cylinders single-acting; power, speed, and pulsations exhibit substantial modulation with typical period of five seconds; the power modulation range exceeds 10% of the average power for Cylinder 1.
4. The unsteadiness appears to result from unfiltered pulsations at one times the running speed, combined with a pronounced beating phenomenon.
5. The beating likely results from relatively small speed differences between units connected to a common header. Unit-to-unit phase differences vary with a period of seconds between reinforcement and cancellation of their respective pulsations.
6. The field modifications to the data acquisition software successfully enabled the unsteadiness to be documented and quantified.
7. With all cylinders double-acting, operation becomes much steadier, and power modulations are much reduced; cylinder standard deviation reduces by about 75% to a sum for all cylinders of 6 HP out of 1,200 HP.
8. Isentropic efficiency based on pressure and temperature from permanently installed station instruments was 87.12% with all cylinders double-acting and 84.18% with two cylinders (1 and 4) single-acting.
9. The ratio of power per unit flow (ICHP/MMSCFD) for single-acting conditions relative to double-acting conditions exceeds the theoretical ratio accounting for conditions by up to 7.8%, depending on assumptions.
10. A methodology has been prototyped for distinguishing losses attributable to valve flow resistance, to irreversibility in compression, and to installation losses.
11. This methodology, applied to a number of cylinder ends under double-acting conditions, indicates that valve losses are in the range of 5% to 7%, and installation losses are about 5%.
12. The simulation model for the Air Balance tasks was finally validated to baseline engine test data. This feat was accomplished with the incorporation of data generated from the geometric analysis and flow bench testing during engine disassembly.
13. Development of several conceptual manifold designs was accomplished. The simulation model and other analysis tools are currently being utilized to determine the optimum configurations and potential benefits.

6. REFERENCES

[1] Smalley, A. J., Mauney, D. A., and Ash, D. I., (1997) Final Report PR-15-9529, "Compressor Station Maintenance Cost Analysis," prepared for the Compressor Research Supervisory Committee of PRC *I*nternational, SwRI Project No. 04-7424.

[2] McKee, R. J., Smalley, A. J., Bourn, G. D., and Young, K. N., (2003) "Detecting Deterioration of Compression Equipment by Normalizing Measured Performance Relative to Expected Performance," GMRC Gas Machinery Conference (GMC), Salt Lake City, Utah.

[3] Harris, R. E., Edlund, C. E., Smalley, A. J., and Weilbacher, G., (2000) "Dynamic Crank Web Strain Measurements for Reciprocating Compressors," presented at the GMRC Gas Machinery Conference (GMC), Colorado Springs, Colorado.

[4] Harris, R. E. and Beeson, C. M., (1990) "Channel Resonance Correction for Improved Cylinder Performance and Diagnostic Analyses," Proceedings, PCRC Fifth Annual Reciprocating Machinery Conference, Nashville, Tennessee.

7. LIST OF ACRONYMS AND ABBREVIATIONS

AGA3	Gas Flow Measurement Standard
BDC	Bottom Dead Center
BEI	Manufacturer's Trade Name
BHP	Brake Horsepower
BWR	Benedict, Webb, Rubin
CPR	Combustion Pressure Ratio
CO_2	Carbon Dioxide
DAS	Data Acquisition System
DOE	U.S. Department of Energy
GMC	Gas Machinery Conference
GMRC	Gas Machinery Research Council
GMV	Cooper Engine Model
GMVH	Cooper Engine Model
GMW10	Cooper Engine Model
HBA-6	Clark Engine Model
HBA-6T	Clark Engine Model
HP	Horsepower
ICHP	Indicated Cylinder Horsepower
IRV	Instantaneous Rotational Velocity
KVS	Ingersoll-Rand Engine Model
MMSCFD	Million of Standard Cubic Feet Per Day
NGK	Manufacturer's Trade Name
NO_x	Oxides of Nitrogen
O_2	Oxygen Molecule
PCB	Manufacturer's Trade Name
PSI	Pounds Per Square Inch
PSIA	Lb./Sq. Inch Absolute
PSIG	Pounds Per Square Inch Gauge
PV	Pressure-Volume
RLM	Rod Load Monitor
RPM	Revolutions Per Minute
SDCM	Strain Data Capture Module
SwRI®	Southwest Research Institute®
TCF	Trillion Cubic Feet
TDC	Top Dead Center
TGHP	Theoretical Gas Horsepower
TLA6	Clark Engine Model with Six Power Cylinders
V-10	10-Cylinder Engine with V Configuration